On the approximation of derivative values using a WENO algorithm with progressive order of accuracy close to discontinuities

Sergio Amat[a], Juan Ruiz-Álvarez[a], Chi-Wang Shu[b], Dionisio F. Yáñez[c]

[a]*Departamento de Matemática Aplicada y Estadística, Universidad Politécnica de Cartagena, Cartagena, Spain*
[b]*Division of Applied Mathematics, Brown University, Providence, Rhode Island, USA*
[c]*Departamento de Matemáticas, Facultad de Matemáticas, Universidad de Valencia, Valencia, Spain*

Abstract

In this article we introduce a new WENO algorithm that aims to calculate an approximation to derivative values of a function in a non-regular grid. We adapt the ideas presented in [S. Amat, J. Ruiz, C.-W. Shu and D.F. Yáñez, *A new WENO-*2*r algorithm with progressive order of accuracy close to discontinuities*, SIAM J. Numer. Anal. (2020)] to design the nonlinear weights in a manner that the order of accuracy is maximum in the intervals close to the discontinuities. Some proofs, remarks on the choice of the stencils and explicit formulas for the weights and smoothness indicators are given. We also present some numerical experiments in order to confirm the theoretical results.

Keywords: WENO-2r, high accuracy interpolation, improved adaption to discontinuities, generalization

1. Introduction and review: central WENO and motivation

In this paper, we design a family of central weighted essentially non-oscillatory (CWENO) schemes that allows to approximate derivative values. We are inspired by the algorithm employed by Levy et al. in [9], which is designed to approximate solutions of hyperbolic systems of conservation laws,

$$\begin{cases} u_t + f(u)_x = 0, \quad u \in \mathbb{R}^2, \\ u(x,0) = u_0(x). \end{cases}$$

In our case, the motivation would be the possible application of the new algorithm to obtain approximations of the solution of Hamilton-Jacobi type equations,

$$\begin{cases} \varphi_t + H(\varphi_x) = 0, \\ \varphi(x,0) = \varphi_0(x), \end{cases} \tag{1}$$

where algorithms that use interpolation to get accurate approximations to the derivative φ_x have been proved to be very useful. In what follows, we show the construction of the algorithm and provide theoretical and numerical proofs of its accuracy, but we let the solution of the equation in (1) as future work. Even so, as we show in what follows, the algorithm proposed can be used as a general technique to obtain the derivatives of a function with singularities, providing progressive order of accuracy close to these singularities.

In [9] the authors use a uniform discretization in time but not in space, i.e. $x_i = h_i$ are the spatial grid-points and $t^n = n\Delta t$ are the time steps. In [9], two reconstructions are necessary to design the method: Firstly, a reconstruction scheme to approximate the average of the function u over a cell at a time t^n. Secondly, a reconstruction of f for the derivative of the fluxes, Q_i, which satisfies:

$$\frac{\partial Q_i}{\partial x}(x_i, t^n) =: Q_i'(x_i, t^n) = f'(u(x_i, t^n)) + O(h^{r-1}), \tag{2}$$

*The work of the first and second authors was supported by project 20928/PI/18 (Proyecto financiado por la Comunidad Autónoma de la Región de Murcia a través de la convocatoria de Ayudas a proyectos para el desarrollo de investigación científica y técnica por grupos competitivos, incluida en el Programa Regional de Fomento de la Investigación Científica y Técnica (Plan de Actuación 2018) de la Fundación Séneca-Agencia de Ciencia y Tecnología de la Región de Murcia), by the national research project PID2019-108336GB-I00 (MINECO/FEDER). The work of the third author was supported by NSF grant DMS-2010107 and AFOSR grant FA9550-20-1-0055. The work of the fourth author was supported by Spanish MINECO project MTM2017-83942-P and PID2020-117211GB-I00.

Email addresses: `sergio.amat@upct.es` (Sergio Amat), `juan.ruiz@upct.es` (Juan Ruiz-Álvarez), `chi-wang_shu@brown.edu` (Chi-Wang Shu), `dionisio.yanez@uv.es` (Dionisio F. Yáñez)

where $r-1$ is the accuracy attained for the reconstruction of the derivative, and supposing that u at a time t^n is known. WENO nonlinear interpolation methods can be used for this purpose (see e.g. [9, 10, 11]). In [9], a symmetric strategy is used, but in this work, we construct a general method that is not necessarily symmetric. Therefore, in this paper, we will construct a new non-linear method to approximate the derivative point-values with progressive order of accuracy close to the discontinuities adapting the ideas presented in [3]. We will present this method for any r. We reformulate this problem as follows:

We suppose $[a,b]\subset\mathbb{R}$ and a grid $X=\{x_j\}_{j=0}^J$, $x_0=a,\ x_J=b,\ x_{j+1}=x_j+h_j$, $x_{j+1/2}=x_j+h_j/2$, $x_{j-1/2}=x_j-h_{j-1}/2$, $h=\max\{h_j: j=0,\dots,J-1\}$, and we suppose that there exists $L>0$ such that

$$\widetilde{h}=\frac{\max\{h_j: j=0,\dots,J-1\}}{\min\{h_j: j=0,\dots,J-1\}}=\frac{h}{\min\{h_j: j=0,\dots,J-1\}}\leq L.$$

For a piecewise smooth function f we consider a point value discretization $f(x_j)=f_j,\ j=0,\dots,J$. In order to calculate the derivative value at a specific point x_i, we take the stencils of r points which contain it, i.e. let $\mathcal{I}^r_{i,k}=\{i-(r-1)+k,\dots,i+k\}$ be the subindex and the stencils $\mathcal{S}^r_{i,k}=\{x_t: t\in\mathcal{I}^i_k\}$ with $k=0,\dots,r-1$ and calculate the interpolation polynomial of degree $r-1$ such that $p^{r-1}_{i,k}(x_j)=f_j,\ j\in\mathcal{I}^r_{i,k}$. The classic WENO interpolator is a convex combination of these polynomials:

$$P_i(x)=\sum_{k=0}^{r-1}\omega^{r-1}_{i,k}p^{r-1}_{i,k}(x),$$

where $\omega^{r-1}_{i,k}$ are nonlinear weights whose value depends on the existence of a discontinuity affecting the stencil. In our case, we will define

$$(P_i)'(x_i)=\frac{dP_i}{dx}(x_i)=\sum_{k=0}^{r-1}\omega^{r-1}_{i,k}\frac{dp^{r-1}_{i,k}}{dx}(x_i). \tag{3}$$

It is clear that if the function is smooth at the largest stencil $\{x_{i-(r-1)},\dots,x_{i+(r-1)}\}$, then, if the choice of the nonlinear weights is adequate, we can obtain an approximation of the derivative values of order of accuracy $O(h^{2r-2})$. However, when a discontinuity crosses the above mentioned stencil, typically (see, e.g. [10]) , the order decreases to $r-1$. Note that there are two principal differences between classical WENO interpolation for point-value approximation of a function and the WENO algorithm used to obtain an approximation of the derivative values:

1. When we use classical WENO algorithm for point-value interpolation, we take the stencils which contain x_{i-1} and x_i because, typically, we interpolate at $x_{i-\frac{1}{2}}$.

2. The evaluation of the derivative of the polynomial, P_i', Eq. (3), is at x_i not at $x_{i-\frac{1}{2}}$.

The key of this method is the definition of the nonlinear weights, that make use of linear optimal weights and that are defined as follows. Let $p^{2r-2}_{i,0}$ be the polynomial which interpolates f at $\{x_{i-(r-1)},\dots,x_{i+(r-1)}\}$, then there exist $C^{r-1}_{i,k}>0$, $k=0,\dots,r-1$ which satisfy:

$$\frac{dp^{2r-2}_{i,0}}{dx}(x_i)=\sum_{k=0}^{r-1}C^{r-1}_{i,k}\frac{dp^{r-1}_{i,k}}{dx}(x_i),\qquad \sum_{k=0}^{r-1}C^{r-1}_{i,k}=1. \tag{4}$$

The following proposition for non-uniform grid is proved in [12] using the ideas proposed in [6]. We reproduce it here for completeness.

Proposition 1.1. *The optimal weights are determined by:*

$$\begin{aligned}
C^{r-1}_{i,0}&=\prod_{s=i+1}^{i+(r-1)}\frac{x_i-x_s}{x_{i-(r-1)}-x_s},\\
C^{r-1}_{i,k}&=\prod_{s\in\mathcal{I}^{2r-1}_{i,0}\setminus\mathcal{I}^r_{i,k}}\frac{x_i-x_s}{x_{i-(r-1)+k}-x_s}-\sum_{t=0}^{k-1}C^{r-1}_{i,t}\prod_{s\in\mathcal{I}^r_{i,t}\setminus\mathcal{I}^r_{i,k}}\frac{x_i-x_s}{x_{i-(r-1)+k}-x_s}\prod_{s\in\mathcal{I}^r_{i,k}\setminus\mathcal{I}^r_{i,t}}\frac{x_{i-(r-1)+k}-x_s}{x_i-x_s},
\end{aligned} \tag{5}$$

with $0\leq k<r-1$.

Proof. Using Lagrange's base, we know that:

$$L_{j,k}^{r-1}(x) = \prod_{\substack{t=i-(r-1)+k \\ t\neq j}}^{i+k} \frac{x-x_t}{x_j-x_t},$$

then:

$$p_{i,k}^{r-1}(x) = \sum_{j=i-(r-1)+k}^{i+k} f_j L_{j,k}^{r-1}(x) \to \frac{d}{dx} p_{i,k}^{r-1}(x) = \sum_{j=i-(r-1)+k}^{i+k} f_j \frac{d}{dx} L_{j,k}^{r-1}(x),$$

with

$$\frac{d}{dx} L_{j,k}^{r-1}(x) = \sum_{s=i-(r-1)+k}^{i+k} \frac{1}{x_j-x_s} \prod_{\substack{t=i-(r-1)+k \\ t\neq j,s}}^{i+k} \frac{x-x_t}{x_j-x_t}.$$

Therefore:

$$\frac{d}{dx} p_{i,k}^{r-1}(x_i) = \sum_{\substack{j=i-(r-1)+k \\ j\neq i}}^{i+k} \left(\frac{f_i}{x_i-x_j} + \frac{f_j}{x_j-x_i} \prod_{\substack{s=i-(r-1)+k \\ s\neq i,j}}^{i+k} \frac{x_i-x_s}{x_j-x_s} \right) = \sum_{j\in \mathcal{I}_{i,k}^r \setminus\{i\}} \left(\frac{f_i}{x_i-x_j} + \frac{f_j}{x_j-x_i} \prod_{s\in \mathcal{I}_{i,k}^r \setminus\{i,j\}} \frac{x_i-x_s}{x_j-x_s} \right).$$

Analogously:

$$\frac{d}{dx} p_{i,0}^{2r-2}(x_i) = \sum_{j\in \mathcal{I}_{i,0}^{2r-1} \setminus\{i\}} \left(\frac{f_i}{x_i-x_j} + \frac{f_j}{x_j-x_i} \prod_{s\in \mathcal{I}_{i,0}^{2r-1} \setminus\{i,j\}} \frac{x_i-x_s}{x_j-x_s} \right).$$

We can obtain the optimal weights from the equality:

$$\frac{d}{dx} p_{i,0}^{2r-2}(x_i) = \sum_{k=0}^{r-1} C_{i,k}^{r-1} \frac{d}{dx} p_{i,k}^{r-1}(x_i), \tag{6}$$

thus, if $k=0$ then the unique stencil of r points which contains the point $x_{i-(r-1)}$ is $\mathcal{S}_{i,0}^r$. Then, taking the term of $f_{i-(r-1)}$, we obtain:

$$\frac{C_{i,0}^{r-1}}{x_{i-(r-1)}-x_i} \prod_{s=i-(r-1)+1}^{i-1} \frac{x_i-x_s}{x_{i-(r-1)}-x_s} = \frac{1}{x_{i-(r-1)}-x_i} \prod_{\substack{s=i-(r-1)+1 \\ s\neq i}}^{i+(r-1)} \frac{x_i-x_s}{x_{i-(r-1)}-x_s} \to C_{i,0}^{r-1} = \prod_{s=i+1}^{i+(r-1)} \frac{x_i-x_s}{x_{i-(r-1)}-x_s}.$$

Now, if we take $k=1$ we have only two *stencils*: $\mathcal{S}_{i,0}^r$ and $\mathcal{S}_{i,1}^r$ which contain the point $x_{i-(r-1)+1}$. Then using Eq. (6) at term $f_{i-(r-1)+1}$, we get:

$$\frac{C_{i,0}^{r-1}}{x_{i-(r-1)+1}-x_i} \prod_{\substack{s=i-(r-1) \\ s\neq i-(r-1)+1}}^{i-1} \frac{x_i-x_s}{x_{i-(r-1)+1}-x_s} + \frac{C_{i,1}^{r-1}}{x_{i-(r-1)+1}-x_i} \prod_{\substack{s=i-(r-1)+2 \\ s\neq i}}^{i+1} \frac{x_i-x_s}{x_{i-(r-1)+1}-x_s} =$$

$$= \frac{1}{x_{i-(r-1)+1}-x_i} \prod_{\substack{s=i-(r-1) \\ s\neq i,i-(r-1)+1}}^{i+(r-1)} \frac{x_i-x_s}{x_{i-(r-1)+1}-x_s},$$

$$C_{i,1}^{r-1} = \prod_{\mathcal{I}_{i,0}^{2r-1} \setminus \mathcal{I}_{i,1}^r} \frac{x_j-x_k}{x_{j-r+1}-x_k} - C_{i,0}^{r-1} \prod_{s\in \mathcal{I}_{i,0}^r \setminus \mathcal{I}_{i,1}^r} \frac{x_i-x_s}{x_{i-(r-1)+1}-x_s} \prod_{s\in \mathcal{I}_{i,1}^r \setminus \mathcal{I}_{i,0}^r} \frac{x_{i-(r-1)+1}-x_s}{x_i-x_s}.$$

We suppose that we have obtained the optimal weights $C_{i,0}^{r-1}, C_{i,1}^{r-1}, \dots, C_{i,k-1}^{r-1}$ with $0<k<r-1$, we will get $C_{i,k}^{r-1}$. The point $x_{i-(r-1)+k}$ is in the *stencils* $\mathcal{S}_{i,0}^r, \mathcal{S}_{i,1}^r, \dots, \mathcal{S}_{i,k}^r$, then for the term $f_{i-(r-1)+k}$ in Eq. (6) we get:

$$\sum_{t=0}^{k} \frac{C_{i,t}^{r-1}}{x_{i-(r-1)+k}-x_i} \prod_{s\in \mathcal{I}_{i,t}^r \setminus\{i,i-(r-1)+k\}} \frac{x_i-x_s}{x_{i-(r-1)+k}-x_s} = \frac{1}{x_{i-(r-1)+k}-x_i} \prod_{s\in \mathcal{I}_{i,0}^{2r-1} \setminus\{i,i-(r-1)+k\}} \frac{x_i-x_s}{x_{i-(r-1)+k}-x_i}.$$

Then,

$$C_{i,k}^{r-1} = \prod_{s\in\mathcal{I}_{i,0}^{2r-1}\setminus\mathcal{I}_{i,k}^{r}} \frac{x_i - x_s}{x_{i-(r-1)+k} - x_s} - \sum_{t=0}^{k-1} C_{i,t}^{r-1} \prod_{s\in\mathcal{I}_{i,t}^{r}\setminus\mathcal{I}_{i,k}^{r}} \frac{x_i - x_s}{x_{i-(r-1)+k} - x_s} \prod_{s\in\mathcal{I}_{i,k}^{r}\setminus\mathcal{I}_{i,t}^{r}} \frac{x_{i-(r-1)+k} - x_s}{x_i - x_s}.$$

■

In Tables 1 and 2 we show the values $C_{i,k}^{r-1}$, $0 \leq k \leq r-1$ for $r = 2, 3$ and 4.

	$r=2$	$r=3$
$C_{i,0}^{r-1}$	$\frac{x_{i+1}-x_i}{x_{i+1}-x_{i-1}}$	$\frac{(x_i-x_{i+1})(x_i-x_{i+2})}{(x_{i-2}-x_{i+1})(x_{i-2}-x_{i+2})}$
$C_{i,1}^{r-1}$	$\frac{x_i-x_{i-1}}{x_{i+1}-x_{i-1}}$	$\frac{(x_i-x_{i-2})(x_i-x_{i+2})}{x_{i-2}-x_{i+2}}\left(\frac{1}{x_{i-1}-x_{i+2}}+\frac{1}{x_{i-2}-x_{i+1}}\right)$
$C_{i,2}^{r-1}$		$\frac{(x_i-x_{i-2})(x_i-x_{i-1})}{(x_{i+2}-x_{i-2})(x_{i+2}-x_{i-1})}$

Table 1: Optimal weights for $r = 2, 3$ and a uniform grid.

	$r=4$
$C_{i,0}^{r-1}$	$\frac{(x_i-x_{i+1})(x_i-x_{i+2})(x_i-x_{i+3})}{(x_{i+1}-x_{i-3})(x_{i-3}-x_{i+2})(x_{i+3}-x_{i-3})}$
$C_{i,1}^{r-1}$	$\frac{(x_i-x_{i+2})(x_i-x_{i+3})(x_i-x_{i-3})\big(x_{i+1}(x_{i+2}+x_{i+3}-x_{i-2}-x_{i-3})+x_{i+2}(x_{i+3}-x_{i-2}-x_{i-3})-x_{i+3}x_{i-2}-x_{i+3}x_{i-3}+x_{i-2}^2+x_{i-2}x_{i-3}+x_{i-3}^2\big)}{(x_{i-3}-x_{i+1})(x_{i+2}-x_{i-2})(x_{i+2}-x_{i-3})(x_{i-2}-x_{i+3})(x_{i+3}-x_{i-3})}$
$C_{i,2}^{r-1}$	$\frac{(x_i-x_{i+3})(x_i-x_{i-2})(x_i-x_{i-3})\big(x_{i+2}^2+x_{i+2}(x_{i+3}-x_{i-1}-x_{i-2}-x_{i-3})+x_{i+3}^2-x_{i+3}(x_{i-1}+x_{i-2}+x_{i-3})+x_{i-1}x_{i-2}+x_{i-1}x_{i-3}+x_{i-2}x_{i-3}\big)}{(x_{i-2}-x_{i+2})(x_{i+2}-x_{i-3})(x_{i+3}-x_{i-1})(x_{i+3}-x_{i-2})(x_{i+3}-x_{i-3})}$
$C_{i,3}^{r-1}$	$\frac{(x_i-x_{i-1})(x_i-x_{i-2})(x_i-x_{i-3})}{(x_{i+3}-x_{i-1})(x_{i+3}-x_{i-2})(x_{i+3}-x_{i-3})}$

Table 2: Optimal weights for $r = 4$ and a non-uniform grid.

If we take a uniform grid, the following corollary is a direct consequence by Prop. 1.1. We denote as $C_{i,k}^{r-1}=C_k^{r-1}$ because this value does not depend on the position i.

Corollary 1.2. *Using a uniform grid, the optimal weights for the approximation of derivative values are given by:*

$$C_k^{r-1}=\binom{r-1}{k}^2\binom{2r-2}{r-1}^{-1},\quad k=0,\cdots,r-1. \tag{7}$$

Proof. From $x_i=ih$, using the Lagrange basis we have that

$$L_{j,k}^{r-1}(x)=\prod_{\substack{s=i-(r-1)+k\\ s\neq i}}^{i+k}\frac{x-sh}{(j-s)h}\quad\to\quad p_k^{r-1}(x)=\sum_{j=i-(r-1)+k}^{i+k}f_jL_{j,k}^{r-1}(x)\to$$
$$\frac{d}{dx}p_k^{r-1}(x_i)=\sum_{\substack{j=i-(r-1)+k\\ j\neq i}}^{i+k}\left(\frac{f_i}{(i-j)h}+\frac{f_j}{(j-i)h}\prod_{\substack{s=i-(r-1)+k\\ s\neq i,j}}^{i+k}\frac{i-s}{j-s}\right).$$

Analogously

$$\frac{d}{dx}p_0^{2r-2}(x_i)=\sum_{\substack{j=i-(r-1)\\ j\neq i}}^{i+(r-1)}\left(\frac{f_i}{(i-j)h}+\frac{f_j}{(j-i)h}\prod_{\substack{s=i-(r-1)\\ s\neq i,j}}^{i+(r-1)}\frac{i-s}{j-s}\right).$$

By induction on k, if $k=0$ and $\xi=s-i$ then

$$C_0^{r-1}\frac{f_{i-(r-1)}}{-(r-1)h}\prod_{s=i-(r-1)+1}^{i}\frac{i-s}{i-(r-1)-s}=\frac{f_{i-(r-1)}}{-(r-1)h}\prod_{s=i-(r-1)+1}^{i+(r-1)}\frac{i-s}{i-(r-1)-s}\to$$
$$C_0^{r-1}=\prod_{s=i+1}^{i+(r-1)}\frac{i-s}{i-(r-1)-s}=\prod_{s=i+1}^{i+(r-1)}\frac{s-i}{s-i+(r-1)}=\prod_{\xi=1}^{r-1}\frac{\xi}{\xi+(r-1)}=\binom{2r-2}{r-1}^{-1}.$$

We suppose the result for $k-1$ and calculate C_k^{r-1}, with $0\le t<k\le r-1$. Thus, since

$$\begin{aligned}\mathcal{I}_{i,0}^{2r-1}\setminus\mathcal{I}_{i,k}^{r}&=\{i-(r-1),i-(r-1)+1,\dots,i-(r-1)+k-1,i+k+1,\dots,i+(r-1)\},\\ \mathcal{I}_{i,k}^{r}\setminus\mathcal{I}_{i,t}^{r}&=\{i+t+1,\dots,i+k\},\\ \mathcal{I}_{i,t}^{r}\setminus\mathcal{I}_{i,k}^{r}&=\{i-(r-1)+t,\dots,i-(r-1)+k-1\},\end{aligned} \tag{8}$$

we obtain:

$$\begin{aligned}\prod_{s\in\mathcal{I}_{i,0}^{2r-1}\setminus\mathcal{I}_{i,k}^{r}}\frac{x_i-x_s}{x_{i-(r-1)+k}-x_s}&=\prod_{s=i-(r-1)}^{i-(r-1)+k-1}\frac{x_i-x_s}{x_{i-(r-1)+k}-x_s}\prod_{s=i+k+1}^{i+(r-1)}\frac{x_i-x_s}{x_{i-(r-1)+k}-x_s}\\ &=\prod_{l=0}^{k-1}\frac{(r-1)-l}{k-l}\prod_{l=k+1}^{r-1}\frac{l}{l+(r-1)-k}=\binom{r-1}{k}\binom{2(r-1)}{r-1}^{-1}\binom{2(r-1)}{k},\\ \prod_{s\in\mathcal{I}_{i,k}^{r}\setminus\mathcal{I}_{i,t}^{r}}\frac{x_i-x_s}{x_{i-(r-1)+k}-x_s}&=\prod_{s=i+t+1}^{i+k}\frac{x_i-x_s}{x_{i-(r-1)+k}-x_s}=\prod_{l=t+1}^{k}\frac{l}{l+(r-1)-k}=\frac{k!((r-1)-(k-t))!}{(r-1)!t!},\\ &=\frac{k!((r-1)-(k-t))!(k-t)!}{(r-1)!t!(k-t)!}=\binom{k}{t}\binom{r-1}{k-t}^{-1},\\ \prod_{s\in\mathcal{I}_{i,t}^{r}\setminus\mathcal{I}_{i,k}^{r}}\frac{x_i-x_s}{x_{i-(r-1)+k}-x_s}&=\prod_{s=i-(r-1)+t}^{i-(r-1)+k-1}\frac{x_i-x_s}{x_{i-(r-1)+k}-x_s}=\prod_{l=t}^{k-1}\frac{(r-1)-l}{k-l}=\binom{r-1}{k}\binom{r-1}{t}^{-1}\binom{k}{t},\end{aligned} \tag{9}$$

Then, since

$$\binom{2(r-1)}{k} - \sum_{t=0}^{k-1} \binom{r-1}{t}\binom{r-1}{k-t} = \binom{r-1}{k},$$

by induction hypothesis, by (9) and by Prop. 1.1, we have:

$$\begin{aligned}
C_k^{r-1} &= \prod_{s\in \mathcal{I}_{i,0}^{2r-1}\setminus \mathcal{I}_k^r} \frac{x_i - x_s}{x_{i-(r-1)+k} - x_s} - \sum_{t=0}^{k-1} C_t^{r-1} \prod_{s\in \mathcal{I}_{i,t}^r\setminus \mathcal{I}_{i,k}^r} \frac{x_i - x_s}{x_{i-(r-1)+k} - x_s} \prod_{s\in \mathcal{I}_{i,k}^r\setminus \mathcal{I}_{i,t}^r} \frac{x_{i-(r-1)+k} - x_s}{x_i - x_s} \\
&= \binom{r-1}{k}\binom{2(r-1)}{r-1}^{-1}\binom{2(r-1)}{k} - \sum_{t=0}^{k-1}\binom{r-1}{t}^2\binom{2r-2}{r-1}^{-1}\binom{r-1}{k}\binom{r-1}{t}^{-1}\binom{k}{t}\binom{k}{t}^{-1}\binom{r-1}{k-t} \\
&= \binom{r-1}{k}\binom{2(r-1)}{r-1}^{-1}\left(\binom{2(r-1)}{k} - \sum_{t=0}^{k-1}\binom{r-1}{t}\binom{r-1}{k-t}\right) = \binom{r-1}{k}^2\binom{2(r-1)}{r-1}^{-1}.
\end{aligned}$$

■

In Table 3 some optimal weights are shown. For $r = 3$, they are the optimal weights showed in [9].

	C_0^{r-1}	C_1^{r-1}	C_2^{r-1}	C_3^{r-1}	C_4^{r-1}
$r = 2$	1/2	1/2	-	-	-
$r = 3$	1/6	2/3	1/6	-	-
$r = 4$	1/20	9/20	9/20	1/20	-
$r = 5$	1/70	8/35	18/35	8/35	1/70

Table 3: Optimal weights $r = 2, 3, 4, 5$ for a uniform grid.

With these linear weights, we can use the following expressions for the nonlinear weights,

$$\omega_{i,k}^{r-1} = \frac{\alpha_{i,k}^{r-1}}{\sum_{j=0}^{r-1}\alpha_{i,j}^{r-1}}, \quad \text{where} \quad \alpha_{i,k}^{r-1} = \frac{C_{i,k}^{r-1}}{(\epsilon + I_{i,k}^{r-1})^{\theta}}, \quad k = 0, \cdots, r-1, \tag{10}$$

with $\sum_{k=0}^{r-1}\omega_{i,k}^{r-1} = 1$. In Eq. (10), the parameter θ is an integer that assures maximum order of accuracy close to the discontinuities, in our case we will take $\theta \geq r$ and the parameter $\epsilon > 0$ is introduced to avoid divisions by zero, we will set it to $\epsilon = 10^{-16}$. The values $I_{i,k}^{r-1}$ are called *smoothness indicators* for $f(x)$ on each sub-stencil of $r-1$ points. There exist several expressions for $I_{i,k}^{r-1}$. For example, the indicators designed in [8] and [9], which are

$$\tilde{I}_{i,k}^{r-1} = \sum_{l=1}^{r-1}(x_{i+1/2} - x_{i-1/2})^{2l-1}\int_{x_{i-1/2}}^{x_{i+1/2}}\left(\frac{d^l}{dx^l}p_{i,k}^{r-1}(x)\right)^2 dx. \tag{11}$$

These indicators are suitable for the approximation of the conservation laws (1) with discontinuities in their solutions. The results obtained using them for approximating the derivative values are not satisfactory because they do not correctly detect kink discontinuities. For approximating the derivative values, suitable for the approximation of the Hamilton-Jacobi equations (1), the measurement of the smoothness indicators should start from the second derivative [7, 2]. In this work, we use the formula given in [2] adapted to non-uniform grids:

$$I_{i,k}^{r-1} = \sum_{l=2}^{r-1}(x_{i+1/2} - x_{i-1/2})^{2l-1}\int_{x_{i-1/2}}^{x_{i+1/2}}\left(\frac{d^l}{dx^l}p_{i,k}^{r-1}(x)\right)^2 dx. \tag{12}$$

Recently, a new WENO-$2r$ algorithm has been introduced in [3, 4]. It consists on exploiting a recursive process to calculate the nonlinear weights with the aim of obtaining progressive order of accuracy of the approximation close to discontinuities. In this paper, we adapt these ideas to obtain a new progressive WENO interpolator to approximate the derivative values. The paper is divided in the following sections: in Section 2 we show the algorithm and construct the new method for $r = 3$ and for $r = 4$. In Section 3, we generalise the results for any r and we give a general expression for non-linear optimal weights. In Section 4, we present a strategy to compute efficiently the smoothness indicators and we study the order of accuracy. Finally, some numerical experiments and some conclusions are presented.

2. New WENO with progressive adaptation to discontinuities: cases $r = 3$ and $r = 4$

The new algorithm designed by Amat et al. in [3] consists on using the Aitken's interpolation process [1] to calculate progressive linear weights. For simplicity, we present two examples and in next section we show the generalization for any r.

2.1. New WENO for $r = 3$ with progressive adaptation to discontinuities in non-uniform grids

Let $p^4_{i,0}$ be the polynomial which interpolates $\{x_{i-2}, x_{i-1}, x_i, x_{i+1}, x_{i+2}\}$, then it can be divided in two polynomials $p^3_{i,0}$ interpolating in $\{x_{i-2}, x_{i-1}, x_i, x_{i+1}\}$ and $p^3_{i,1}$ in $\{x_{i-1}, x_i, x_{i+1}, x_{i+2}\}$. Therefore, by Aitken's process, we have that

$$p^4_{i,0}(x) = C^3_{i,0,0}(x)p^3_{i,0}(x) + C^3_{i,0,1}(x)p^3_{i,1}(x) = \frac{x - x_{i+2}}{x_{i-2} - x_{i+2}} p^3_{i,0}(x) + \frac{x - x_{i-2}}{x_{i+2} - x_{i-2}} p^3_{i,1}(x),$$

then as $p^3_{i,0}$ and $p^3_{i,1}$ interpolate f at x_i, i.e., $p^3_{i,0}(x_i) = p^3_{i,1}(x_i) = f_i$, we have that:

$$\begin{aligned}
\frac{dp^4_{i,0}}{dx}(x) &= \frac{dC^3_{i,0,0}}{dx}(x)p^3_{i,0}(x) + C^3_{i,0,1}(x)\frac{dp^3_{i,0}}{dx}(x) + \frac{dC^3_{i,0,1}(x)}{dx}p^3_{i,1}(x) + C^3_{i,0,1}(x)\frac{dp^3_{i,1}}{dx}(x) \\
&= \frac{1}{(x_{i+2} - x_{i-2})}(p^3_{i,1}(x) - p^3_{i,0}(x)) - \left(\frac{x - x_{i+2}}{x_{i+2} - x_{i-2}}\right)\frac{dp^3_{i,0}}{dx}(x) + \left(\frac{x - x_{i-2}}{x_{i+2} - x_{i-2}}\right)\frac{dp^3_{i,1}}{dx}(x) \rightarrow \\
\frac{dp^4_{i,0}}{dx}(x_i) &= \left(\frac{x_{i+2} - x_i}{x_{i+2} - x_{i-2}}\right)\frac{dp^3_{i,0}}{dx}(x_i) + \left(\frac{x_i - x_{i-2}}{x_{i+2} - x_{i-2}}\right)\frac{dp^3_{i,1}}{dx}(x_i).
\end{aligned}$$

Analogously,

$$\begin{aligned}
\frac{dp^3_{i,0}}{dx}(x_i) &= \left(\frac{x_{i+1} - x_i}{x_{i+1} - x_{i-2}}\right)\frac{dp^2_{i,0}}{dx}(x_i) + \left(\frac{x_i - x_{i-2}}{x_{i+1} - x_{i-2}}\right)\frac{dp^2_{i,1}}{dx}(x_i), \\
\frac{dp^3_{i,1}}{dx}(x_i) &= \left(\frac{x_{i+2} - x_i}{x_{i+2} - x_{i-1}}\right)\frac{dp^2_{i,1}}{dx}(x_i) + \left(\frac{x_i - x_{i-1}}{x_{i+2} - x_{i-1}}\right)\frac{dp^2_{i,2}}{dx}(x_i).
\end{aligned}$$

Then, it is clear that:

$$\begin{aligned}
\mathbf{C}^2_i &= (C^2_{i,0}, C^2_{i,1}, C^2_{i,2}) = C^3_{i,0,0}(C^2_{i,0,0}, C^2_{i,0,1}, 0) + C^3_{i,0,1}(0, C^2_{i,1,1}, C^2_{i,1,2}) \\
&= \left(\frac{x_{i+2} - x_i}{x_{i+2} - x_{i-2}}\right)\left(\left(\frac{x_{i+1} - x_i}{x_{i+1} - x_{i-2}}\right), \left(\frac{x_i - x_{i-2}}{x_{i+1} - x_{i-2}}\right), 0\right) + \left(\frac{x_i - x_{i-2}}{x_{i+2} - x_{i-2}}\right)\left(0, \left(\frac{x_{i+2} - x_i}{x_{i+2} - x_{i-1}}\right), \left(\frac{x_i - x_{i-1}}{x_{i+2} - x_{i-1}}\right)\right),
\end{aligned}$$

then, we define:

$$\tilde{\mathbf{C}}^2_i = (\tilde{C}^2_{i,0}, \tilde{C}^2_{i,1}, \tilde{C}^2_{i,2}) = \tilde{\omega}^3_{i,0,0}(C^2_{i,0,0}, C^2_{i,0,1}, 0) + \tilde{\omega}^3_{i,0,1}(0, C^2_{i,1,1}, C^2_{i,1,2}),$$

where

$$\tilde{\omega}^3_{i,0,0} = \frac{\tilde{\alpha}^3_{i,0,0}}{\tilde{\alpha}^3_{i,0,0} + \tilde{\alpha}^3_{i,0,1}}, \quad \tilde{\omega}^3_{i,0,1} = \frac{\tilde{\alpha}^3_{i,0,1}}{\tilde{\alpha}^3_{i,0,0} + \tilde{\alpha}^3_{i,0,1}}, \tag{13}$$

with

$$\tilde{\alpha}^3_{i,0,0} = \frac{C^3_{i,0,0}}{(\epsilon + I^3_{i,0,0})^\theta}, \quad \tilde{\alpha}^3_{i,0,1} = \frac{C^3_{i,0,1}}{(\epsilon + I^3_{i,0,1})^\theta}, \tag{14}$$

where the smoothness indicators $I^3_{i,0,k_1}$, $k_1 = 0, 1$ in (14) will be defined in Section 4 based on those introduced in [9]. Finally, we apply WENO with the new nonlinear weights, i.e., we calculate:

$$\tilde{P}'_i(x_i) = \sum_{k=0}^{2} \tilde{\omega}^2_{i,k}\frac{dp^2_{i,k}}{dx}(x_i), \quad \text{with} \quad \tilde{\omega}^2_{i,k} = \frac{\tilde{\alpha}^2_{i,k}}{\sum_{j=0}^2 \tilde{\alpha}_{i,j}}, \quad \text{and} \quad \tilde{\alpha}^2_{i,k} = \frac{\tilde{C}^2_{i,k}}{(\epsilon + I^2_{i,k})^\theta}, \quad k = 0, 1, 2,$$

being $I^2_{i,k}$, $k = 0, 1, 2$, the smoothness indicators introduced in Eq. (11).

Using the same reasoning, as a corollary, we obtain the formulas for new nonlinear weights in the uniform grid case. Thus, we have that

$$\begin{aligned}
\frac{dp_0^4}{dx}(x) &= \frac{dC_{0,0}^3}{dx}(x)p_0^3(x) + C_{0,1}^3(x)\frac{dp_0^3}{dx}(x) + \frac{dC_{0,1}^3(x)}{dx}p_1^3(x) + C_{0,1}^3(x)\frac{dp_1^3}{dx}(x)\\
&= \frac{1}{4h}(p_1^3(x) - p_0^3(x)) - \left(\frac{x-(i+2)h-a}{4h}\right)\frac{dp_0^3}{dx}(x) + \left(\frac{x-(i-2)h-a}{4h}\right)\frac{dp_1^3}{dx}(x) \to\\
\frac{dp_0^4}{dx}(x_i) &= \frac{1}{2}\frac{dp_0^3}{dx}(x_i) + \frac{1}{2}\frac{dp_1^3}{dx}(x_i),\\
\frac{dp_0^3}{dx}(x_i) &= \frac{1}{3}\frac{dp_0^2}{dx}(x_i) + \frac{2}{3}\frac{dp_1^2}{dx}(x_i), \quad \frac{dp_1^3}{dx}(x_i) = \frac{2}{3}\frac{dp_1^2}{dx}(x_i) + \frac{1}{3}\frac{dp_2^2}{dx}(x_i).
\end{aligned}$$

In this case, we will write $C_{k_2,k_3}^{k_1}(x_i) = C_{k_2,k_3}^{k_1}$ for any k_1, k_2, k_3. Thus, we get:

$$\mathbf{C}^2 = (C_0^2, C_1^2, C_2^2) = C_{0,0}^3(C_{0,0}^2, C_{0,1}^2, 0) + C_{0,1}^3(0, C_{1,1}^2, C_{1,2}^2) = \frac{1}{2}\left(\frac{1}{3}, \frac{2}{3}, 0\right) + \frac{1}{2}\left(0, \frac{2}{3}, \frac{1}{3}\right) = \left(\frac{1}{6}, \frac{2}{3}, \frac{1}{6}\right).$$

We can see that the linear optimal weights, in this case, are similar to the weights shown in [9].

Finally, we repeat the same steps in order to obtain nonlinear weights.

2.2. New WENO with progressive adaptation to discontinuities for $r = 4$ in non-uniform grids

We start with the polynomial $p_{i,0}^6$, which interpolates $\{x_{i-3}, x_{i-2}, x_{i-1}, x_i, x_{i+1}, x_{i+2}, x_{i+3}\}$ and we apply the same process, i.e. we want to express the derivative value of this polynomial at x_i as a combination of the derivative values of the polynomials $p_{i,0}^5$ and $p_{i,1}^5$ at x_i which interpolate at the nodes $\{x_{i-3}, x_{i-2}, x_{i-1}, x_i, x_{i+1}, x_{i+2}\}$ and $\{x_{i-2}, x_{i-2}, x_{i-1}, x_i, x_{i+1}, x_{i+3}\}$ respectively, then, again, using Aitken's algorithm, we obtain:

$$\begin{aligned}
p_{i,0}^6(x) &= \left(\frac{x_{i+3}-x}{x_{i+3}-x_{i-3}}\right)p_{i,0}^5(x) + \left(\frac{x-x_{i-3}}{x_{i+3}-x_{i-3}}\right)p_{i,1}^5(x) \to\\
\frac{dp_{i,0}^6}{dx}(x) &= \left(\frac{1}{x_{i+3}-x_{i-3}}\right)(p_{i,1}^5(x) - p_{i,0}^5(x)) + \left(\frac{x_{i+3}-x}{x_{i+3}-x_{i-3}}\right)\frac{dp_{i,0}^5}{dx}(x) + \left(\frac{x-x_{i-3}}{x_{i+3}-x_{i-3}}\right)\frac{dp_{i,1}^5}{dx}(x) \to\\
\frac{dp_0^6}{dx}(x_i) &= \left(\frac{1}{x_{i+3}-x_{i-3}}\right)(p_{i,1}^5(x_i) - p_{i,0}^5(x_i)) + \left(\frac{x_{i+3}-x_i}{x_{i+3}-x_{i-3}}\right)\frac{dp_{i,0}^5}{dx}(x_i) + \left(\frac{x_i-x_{i-3}}{x_{i+3}-x_{i-3}}\right)\frac{dp_{i,1}^5}{dx}(x_i).
\end{aligned}$$

From $p_{i,1}^5(x_i) = p_{i,0}^5(x_i) = f_i$, we have:

$$\frac{dp_{i,0}^6}{dx}(x_i) = \left(\frac{x_{i+3}-x_i}{x_{i+3}-x_{i-3}}\right)\frac{dp_{i,0}^5}{dx}(x_i) + \left(\frac{x_i-x_{i-3}}{x_{i+3}-x_{i-3}}\right)\frac{dp_{i,1}^5}{dx}(x_i).$$

Analogously, we represent $p_{i,0}^5$ as combination of $p_{i,0}^4$ and $p_{i,1}^4$ as

$$p_{i,0}^5(x) = \left(\frac{x_{i+2}-x}{x_{i+2}-x_{i-3}}\right)p_{i,0}^4(x) + \left(\frac{x-x_{i-3}}{x_{i+2}-x_{i-3}}\right)p_{i,1}^4(x),$$

and repeating the same steps we get:

$$\frac{dp_{i,0}^5}{dx}(x_i) = \left(\frac{x_{i+2}-x_i}{x_{i+2}-x_{i-3}}\right)\frac{dp_{i,0}^4}{dx}(x_i) + \left(\frac{x_i-x_{i-3}}{x_{i+2}-x_{i-3}}\right)\frac{dp_{i,1}^4}{dx}(x_i).$$

We repeat this procedure again to obtain:

$$\begin{aligned}
\frac{dp_{i,1}^5}{dx}(x_i) &= \left(\frac{x_{i+3}-x_i}{x_{i+3}-x_{i-2}}\right)\frac{dp_{i,1}^4}{dx}(x_i) + \left(\frac{x_i-x_{i-2}}{x_{i+3}-x_{i-2}}\right)\frac{dp_{i,2}^4}{dx}(x_i),\\
\frac{dp_{i,0}^4}{dx}(x_i) &= \left(\frac{x_{i+1}-x_i}{x_{i+1}-x_{i-3}}\right)\frac{dp_{i,0}^3}{dx}(x_i) + \left(\frac{x_i-x_{i-3}}{x_{i+1}-x_{i-3}}\right)\frac{dp_{i,1}^3}{dx}(x_i),\\
\frac{dp_{i,1}^4}{dx}(x_i) &= \left(\frac{x_{i+2}-x_i}{x_{i+2}-x_{i-2}}\right)\frac{dp_{i,1}^3}{dx}(x_i) + \left(\frac{x_i-x_{i-2}}{x_{i+2}-x_{i-2}}\right)\frac{dp_{i,2}^3}{dx}(x_i),\\
\frac{dp_{i,2}^4}{dx}(x_i) &= \left(\frac{x_{i+3}-x_i}{x_{i+3}-x_{i-1}}\right)\frac{dp_{i,2}^3}{dx}(x_i) + \left(\frac{x_i-x_{i-1}}{x_{i+3}-x_{i-1}}\right)\frac{dp_{i,3}^3}{dx}(x_i),
\end{aligned}$$

then, the optimal progressive weights are:

$$\begin{aligned}
\mathbf{C}_i^3 =& C^5_{i,0,0}\left(C^4_{i,0,0}\left(C^3_{i,0,0},C^3_{i,0,1},0,0\right)+C^4_{i,0,1}\left(0,C^3_{i,1,1},C^3_{i,1,2},0\right)\right)+C^5_{i,0,1}\left(C^4_{i,1,1}\left(0,C^3_{i,1,1},C^3_{i,1,2},0\right)+C^4_{i,1,2}\left(0,0,C^3_{i,2,2},C^3_{i,2,3}\right)\right)\\
=&\left(\frac{x_{i+3}-x_i}{x_{i+3}-x_{i-3}}\right)\left(\left(\frac{x_{i+2}-x_i}{x_{i+2}-x_{i-3}}\right)\left(\left(\frac{x_{i+1}-x_i}{x_{i+1}-x_{i-3}}\right),\left(\frac{x_i-x_{i-3}}{x_{i+1}-x_{i-3}}\right),0,0\right)+\right.\\
&\left.+\left(\frac{x_i-x_{i-3}}{x_{i+2}-x_{i-3}}\right)\left(0,\left(\frac{x_{i+2}-x_i}{x_{i+2}-x_{i-2}}\right),\left(\frac{x_i-x_{i-2}}{x_{i+2}-x_{i-2}}\right),0\right)\right)+\\
&+\left(\frac{x_i-x_{i-3}}{x_{i+3}-x_{i-3}}\right)\left(\left(\frac{x_{i+3}-x_i}{x_{i+3}-x_{i-2}}\right)\left(0,\left(\frac{x_{i+2}-x_i}{x_{i+2}-x_{i-2}}\right),\left(\frac{x_i-x_{i-2}}{x_{i+2}-x_{i-2}}\right),0\right)+\right.\\
&\left.+\left(\frac{x_i-x_{i-2}}{x_{i+3}-x_{i-2}}\right)\left(0,0,\left(\frac{x_{i+3}-x_i}{x_{i+3}-x_{i-1}}\right),\left(\frac{x_i-x_{i-1}}{x_{i+3}-x_{i-1}}\right)\right)\right).
\end{aligned}$$

Thus, we can define

$$\tilde{\mathbf{C}}_i^3=\tilde\omega^5_{i,0,0}(\tilde\omega^4_{i,0,0}(C^3_{i,0,0},C^3_{i,0,1},0,0)+\tilde\omega^4_{i,0,1}(0,C^3_{i,1,1},C^3_{i,1,2},0))+\tilde\omega^5_{i,0,1}(\tilde\omega^4_{i,1,1}(0,C^3_{i,1,1},C^3_{i,1,2},0)+\tilde\omega^4_{i,1,2}(0,0,C^3_{i,2,2},C^3_{i,2,3}))$$

where

$$\begin{aligned}
\tilde\omega^5_{i,0,0}&=\frac{\tilde\alpha^5_{i,0,0}}{\tilde\alpha^5_{i,0,0}+\tilde\alpha^5_{i,0,1}},\;\tilde\omega^5_{i,0,1}=\frac{\tilde\alpha^5_{i,0,1}}{\tilde\alpha^5_{i,0,0}+\tilde\alpha^5_{i,0,1}},\;\tilde\omega^4_{i,0,0}=\frac{\tilde\alpha^4_{i,0,0}}{\tilde\alpha^4_{i,0,0}+\tilde\alpha^4_{i,0,1}},\\
\tilde\omega^4_{i,0,1}&=\frac{\tilde\alpha^4_{i,0,1}}{\tilde\alpha^4_{i,0,0}+\tilde\alpha^4_{i,0,1}},\;\tilde\omega^4_{i,1,1}=\frac{\tilde\alpha^4_{i,1,1}}{\tilde\alpha^4_{i,1,1}+\tilde\alpha^4_{i,1,2}},\;\tilde\omega^4_{i,1,1}=\frac{\tilde\alpha^4_{i,1,2}}{\tilde\alpha^4_{i,1,1}+\tilde\alpha^4_{i,1,2}},
\end{aligned}$$

being

$$\tilde\alpha^l_{i,k,k_1}=\frac{C^l_{i,k,k_1}}{(\epsilon+I^l_{i,k,k_1})^\theta},$$

with $l=4,5,\ k=0,1,\ k_1=k,k+1$ and with this vector, we apply classical WENO algorithm.

As a corollary, if the grid is uniform we get:

$$\begin{aligned}
&\frac{dp_0^6}{dx}(x_i)=\frac{1}{2}\frac{dp_0^5}{dx}(x_i)+\frac{1}{2}\frac{dp_1^5}{dx}(x_i), &&\frac{dp_0^5}{dx}(x_i)=\frac{2}{5}\frac{dp_0^4}{dx}(x_i)+\frac{3}{5}\frac{dp_1^4}{dx}(x_i), &&\frac{dp_1^5}{dx}(x_i)=\frac{3}{5}\frac{dp_1^4}{dx}(x_i)+\frac{2}{5}\frac{dp_2^4}{dx}(x_i),\\
&\frac{dp_0^4}{dx}(x_i)=\frac{1}{4}\frac{dp_0^3}{dx}(x_i)+\frac{3}{4}\frac{dp_1^3}{dx}(x_i), &&\frac{dp_1^4}{dx}(x_i)=\frac{1}{2}\frac{dp_1^3}{dx}(x_i)+\frac{1}{2}\frac{dp_2^3}{dx}(x_i), &&\frac{dp_2^4}{dx}(x_i)=\frac{3}{4}\frac{dp_2^3}{dx}(x_i)+\frac{1}{4}\frac{dp_3^3}{dx}(x_i).
\end{aligned}$$

Thus, it is easy to check that,

$$\begin{aligned}
\mathbf{C}^3&=C^5_{0,0}\left(C^4_{0,0}\left(C^3_{0,0},C^3_{0,1},0,0\right)+C^4_{0,1}\left(0,C^3_{1,1},C^3_{1,2},0\right)\right)+C^5_{0,1}\left(C^4_{1,1}\left(0,C^3_{1,1},C^3_{1,2},0\right)+C^4_{1,2}\left(0,0,C^3_{2,2},C^3_{2,3}\right)\right)\\
&=\frac{1}{2}\left(\frac{2}{5}\left(\frac{1}{4},\frac{3}{4},0,0\right)+\frac{3}{5}\left(0,\frac{1}{2},\frac{1}{2},0\right)\right)+\frac{1}{2}\left(\frac{3}{5}\left(0,\frac{1}{2},\frac{1}{2},0\right)+\frac{2}{5}\left(0,0,\frac{3}{4},\frac{1}{4}\right)\right)=\left(\frac{1}{20},\frac{9}{20},\frac{9}{20},\frac{1}{20}\right).
\end{aligned}$$

Finally, we perform the same algorithm to obtain the nonlinear weights.

3. General new WENO algorithm for derivative values and general optimal weights

In this section we will generalize the method for any r. In order to compute the linear weights for each "level" we can prove the following lemma following the same ideas as in [3], i.e., using Aitken's process as in Sections 2.1 and 2.2.

Lemma 3.1. *Let $0<r-1\leq l\leq 2r-3$ and $0\leq k\leq (2r-3)-l$. If we denote as $C^l_{i,k,k}$ and $C^l_{i,k,k+1}$ the values which satisfy:*

$$\frac{dp^{l+1}_{i,k}}{dx}(x_i)=C^l_{i,k,k}\frac{dp^l_{i,k}(x_i)}{dx}+C^l_{i,k,k+1}\frac{dp^l_{i,k+1}}{dx}(x_i), \tag{15}$$

then

$$C^l_{i,k,k}=\frac{x_{i-(r-1)+k+l+1}-x_i}{x_{i-(r-1)+k+l+1}-x_{i-(r-1)+k}},\quad C^l_{i,k,k+1}=\frac{x_i-x_{i-(r-1)+k}}{x_{i-(r-1)+k+l+1}-x_{i-(r-1)+k}}. \tag{16}$$

Proof. Let $r-1 \leq l \leq 2r-3$ and $0 \leq k \leq (2r-3)-l$. In order to obtain the interpolators $p^{l+1}_{i,k}$, $p^l_{i,k}$ and $p^l_{i,k+1}$ the stencils used are $\{x_{i-(r-1)+k}, \dots, x_{i-(r-1)+k+l+1}\}$, $\{x_{i-(r-1)+k}, \dots, x_{i-(r-1)+k+l}\}$ and $\{x_{i-(r-1)+k+1}, \dots, x_{i-(r-1)+k+l+1}\}$ respectively. Then, using Aitken's interpolation process [1], we obtain:

$$p^{l+1}_{i,k}(x) = \left(\frac{x_{i-(r-1)+k+l+1} - x}{x_{i-(r-1)+k+l+1} - x_{i-(r-1)+k}}\right) p^l_{i,k}(x) - \left(\frac{x_{i-(r-1)+k} - x}{x_{i-(r-1)+k+l+1} - x_{i-(r-1)+k}}\right) p^l_{i,k+1}(x).$$

If we differentiate the previous expression:

$$\begin{aligned}\frac{dp^{l+1}_{i,k}}{dx}(x) =& \frac{1}{x_{i-(r-1)+k+l+1} - x_{i-(r-1)+k}}(p^l_{i,k+1}(x) - p^l_{i,k}(x)) + \\ &\left(\frac{x_{i-(r-1)+k+l+1} - x}{x_{i-(r-1)+k+l+1} - x_{i-(r-1)+k}}\right)\frac{dp^l_{i,k}}{dx}(x) - \left(\frac{x_{i-(r-1)+k} - x}{x_{i-(r-1)+k+l+1} - x_{i-(r-1)+k}}\right)\frac{dp^l_{i,k+1}}{dx}(x),\end{aligned}$$

since $p^l_{i,k+1}(x_i) = p^l_{i,k}(x_i)$, we get:

$$\frac{dp^{l+1}_{i,k}}{dx}(x_i) = \left(\frac{x_{i-(r-1)+k+l+1} - x_i}{x_{i-(r-1)+k+l+1} - x_{i-(r-1)+k}}\right)\frac{dp^l_{i,k}}{dx}(x_i) + \left(\frac{x_i - x_{i-(r-1)+k}}{x_{i-(r-1)+k+l+1} - x_{i-(r-1)+k}}\right)\frac{dp^l_{i,k+1}}{dx}(x_i).$$

■

It is trivial to check that for all i we have:

$$C^l_{i,k,k} + C^l_{i,k,k+1} = 1,\ 0 < r-1 \leq l \leq 2r-3 \text{ and } 0 \leq k \leq (2r-3)-l.$$

As a corollary, we can calculate the optimal weights if the grid is uniform.

Corollary 3.2. *Let $0 < r-1 \leq l \leq 2r-3$ and $0 \leq k \leq (2r-3)-l$, if the grid is uniform, i.e. there exists $h = 1/J$ such that $x_j = a + j \cdot h$, $0 \leq j \leq J$ and we denote as $C^l_{k,k}$ and $C^l_{k,k+1}$ the values which satisfy:*

$$\frac{dp^{l+1}_k}{dx}(x_i) = C^l_{k,k}\frac{dp^l_k}{dx}(x_i) + C^l_{k,k+1}\frac{dp^l_{k+1}}{dx}(x_i), \tag{17}$$

then

$$C^l_{k,k} = \frac{k-(r-1)+(l+1)}{l+1}, \quad C^l_{k,k+1} = \frac{(r-1)-k}{l+1}. \tag{18}$$

Proof. It is direct by Lemma 3.1 and $x_j = a + j \cdot h$, $0 \leq j \leq J$. ■

We apply Eq. (15) for each level and we get:

$$\begin{aligned}\frac{dp^{2r-2}_{i,0}}{dx}(x_i) &= \sum_{j_0=0}^{1} C^{2r-3}_{i,0,j_0}\frac{dp^{2r-3}_{i,j_0}}{dx}(x_i) = \sum_{j_0=0}^{1} C^{2r-3}_{i,0,j_0}\left(\sum_{j_1=j_0}^{j_0+1} C^{2r-4}_{i,j_0,j_1}\frac{dp^{2r-4}_{i,j_1}}{dx}(x_i)\right) = \dots \\ &= \sum_{j_0=0}^{1} C^{2r-3}_{i,0,j_0}\left(\sum_{j_1=j_0}^{j_0+1} C^{2r-4}_{i,j_0,j_1}\left(\dots\left(\sum_{j_{r-3}=j_{r-4}}^{j_{r-4}+1} C^{r-2}_{i,j_{r-4},j_{r-3}}\left(\sum_{j_{r-2}=j_{r-3}}^{j_{r-3}+1} C^{r-1}_{i,j_{r-3},j_{r-2}}\frac{dp^{r-1}_{i,j_{r-2}}}{dx}(x_i)\right)\dots\right)\right)\right).\end{aligned} \tag{19}$$

Thus, if we define the weights and the vector $\mathbf{C^{r-1}_{i,k}}$ with $0 \leq k \leq r-2$ as

$$\mathbf{C^{r-1}_{i,0}} = \left(C^{r-1}_{i,0,0}, C^{r-1}_{i,0,1}, 0, \dots, 0\right), \mathbf{C^{r-1}_{i,1}} = \left(0, C^{r-1}_{i,1,1}, C^{r-1}_{i,1,2}, 0, \dots, 0\right), \dots, \mathbf{C^{r-1}_{i,r-2}} = \left(0, \dots, 0, C^{r-1}_{i,r-2,r-2}, C^{r-1}_{i,r-2,r-1}\right), \tag{20}$$

where $C^{r-1}_{i,k,k}$, $C^{r-1}_{i,k,k+1}$ are defined in Eq. (16), then we get that:

$$\sum_{j_0=0}^{1} C^{2r-3}_{i,0,j_0}\left(\sum_{j_1=j_0}^{j_0+1} C^{2r-4}_{i,j_0,j_1}\left(\dots\left(\sum_{j_{r-3}=j_{r-4}}^{j_{r-4}+1} C^{r-2}_{i,j_{r-4},j_{r-3}}\mathbf{C^{r-1}_{i,j_{r-3}}}\right)\dots\right)\right) = (C^{r-1}_{i,0}, C^{r-1}_{i,1}, \dots, C^{r-1}_{i,r-1}) = \mathbf{C^{r-1}_i}, \tag{21}$$

being $C^{r-1}_{i,k}$, $0\leq k\leq r-1$ the optimal weights obtained in Prop. 1.1, Tables 1 and 2 for $r=2,3$ and 4. Analogously in uniform grid case.

We have a tree scheme, where each branch produces a polynomial of a determined degree. Now, the idea is to use all the points which are not contaminated by a discontinuity. In order to follow this idea, we reduce this branch to $O(h^2)$ using nonlinear weights as follows:

We substitute in Eq. (21) the linear weights by nonlinear weights

$$\omega^l_{i,k,k_1}=\frac{\alpha^l_{i,k,k_1}}{\alpha^l_{i,k,k}+\alpha^l_{i,k,k+1}},\quad \alpha^l_{i,k,k_1}=\frac{C^l_{i,k,k_1}}{(\epsilon+I^l_{i,k,k_1})^\theta},\quad k_1=k,\ k+1, \tag{22}$$

where θ,ϵ are the parameters above mentioned and I^l_{i,k,k_1} are smoothness indicators defined at level $l=r,\dots,2r-3$. Therefore, the last ingredient of this scheme is to define the indicators in order to "remove" (to obtain $O(h^2)$) the non-suitable branch. We will use the strategy used in [3] explained in detail in Sec. 4.

Finally, we define the new weights as:

$$\tilde{\mathbf{C}}^{\mathbf{r-1}}_{\mathbf{i}}=(\tilde{C}^{r-1}_{i,0},\tilde{C}^{r-1}_{i,1},\dots,\tilde{C}^{r-1}_{i,r-2},\tilde{C}^{r-1}_{i,r-1})=\sum_{j_0=0}^{1}\omega^{2r-3}_{0,j_0}\left(\sum_{j_1=j_0}^{j_0+1}\omega^{2r-4}_{i,j_0,j_1}\left(\cdots\left(\sum_{j_{r-3}=j_{r-4}}^{j_{r-4}+1}\omega^{r-2}_{i,j_{r-4},j_{r-3}}\mathbf{C}^{\mathbf{r-1}}_{\mathbf{i,j_{r-3}}}\right)\cdots\right)\right). \tag{23}$$

Using $\tilde{\mathbf{C}}^{\mathbf{r-1}}_{\mathbf{i}}$, we apply classical WENO and calculate $\tilde{P}'_i(x_i)=\sum_{k=0}^{r-1}\tilde{\omega}^{r-1}_{i,k}\frac{dp^{r-1}_{i,k}}{dx}(x_i)$ with

$$\tilde{\omega}^{r-1}_{i,k}=\frac{\tilde{\alpha}^{r-1}_{i,k}}{\sum_{j=0}^{r-1}\tilde{\alpha}_{i,j}},\quad\text{and}\quad \tilde{\alpha}^{r-1}_{i,k}=\frac{\tilde{C}^{r-1}_{i,k}}{(\epsilon+I^{r-1}_{i,k})^\theta},\quad k=0,\dots,r-1. \tag{24}$$

4. Smoothness indicators and analysis of the accuracy

Let us start with the analysis of the smoothness indicators presented by Amat and Ruiz in [2], Eq. (12):

$$I^{r-1}_{i,k}=\sum_{l=2}^{r-1}(x_{i+1/2}-x_{i-1/2})^{2l-1}\int_{x_{i-1/2}}^{x_{i+1/2}}\left(\frac{d^l}{dx^l}p^{r-1}_{i,k}(x)\right)^2dx=\sum_{l=2}^{r-1}\left(\frac{h_i+h_{i-1}}{2}\right)^{2l-1}\int_{x_{i-1/2}}^{x_{i+1/2}}\left(\frac{d^l}{dx^l}p^{r-1}_{i,k}(x)\right)^2dx,$$

$k=0,\dots,r-1$, in non-uniform grids. We use the same ideas introduced in [6]. First of all, at the smooth zones we obtain $I^{r-1}_{i,k}=O(h^4)$ using the following adapted result proved in [2].

Lemma 4.1. *Let $0\leq k\leq r-1$ and $p^{r-1}_{i,k}$ the interpolating polynomial of degree $r-1\geq 2$ of f that uses the nodes of the stencil $\mathcal{S}^r_{i,k}$. Then, the smoothness indicator obtained through* (11) *satisfy*

$$I^{r-1}_k=\begin{cases}O(h^4), & \text{if } f \text{ is smooth in } \mathcal{S}^r_{i,k},\\ O(h^2), & \text{if } f \text{ has a corner discontinuity in } \mathcal{S}^r_{i,k},\\ O(1), & \text{if } f \text{ is discontinuous in } \mathcal{S}^r_{i,k},\end{cases}$$

being $h=\max\{h_j:j=0,\dots,J-1\}$.

We will prove the following auxiliary lemmas using the ideas presented in [6].

Lemma 4.2. *Let $0\leq k,k_1\leq r-1$ and let $I^{r-1}_{i,n}$, $n=k,k_1$ be smoothness indicators of f on the stencil $\mathcal{S}^r_{i,n}=\{x_{i-(r-1)+n},\cdots,x_{i+n}\}$. If $f\in C^r([x_{i+n-(r-1)},x_{i+n}])$, then*

$$I^{r-1}_{i,k}-I^{r-1}_{i,k_1}=O(h^{r+3}).$$

Proof. Let $p^{r-1}_{i,k}, p^{r-1}_{i,k_1}$ be the two interpolating polynomials of f of degree $r-1 \geq 2$ at nodes in the stencil $\mathcal{S}^r_{i,n}$ $n = k, k_1$. As $k \neq k_1$ and $0 \leq k, k_1 \leq r-1$ then $f \in C^r([x_{i-1}, x_{i+1}])$, if $1 \leq l \leq r-1$, $x \in [x_{i-1/2}, x_{i+1/2}] \subset [x_{i-1}, x_{i+1}]$, we have that $|(p^{r-1}_{i,n}(x) - f(x))^{(l)}| \leq O(h^{r-l})$, and

$$\begin{aligned} \left|(f^{(l)}(x))^2 - ((p^{r-1}_{i,n}(x))^{(l)})^2\right| &= \left|\left(f^{(l)}(x) - (p^{r-1}_{i,n})^{(l)}(x)\right)\left(f^{(l)}(x) + (p^{r-1}_{i,n}(x))^{(l)}\right)\right| \\ &\leq O(h^{r-l})O(1) = O(h^{r-l}). \end{aligned} \tag{25}$$

Therefore, we get

$$\begin{aligned} \left|I^{r-1}_{i,n} - \sum_{l=2}^{r-1}\left(\frac{h_i + h_{i-1}}{2}\right)^{2l-1}\int_{x_{i-1/2}}^{x_{i+1/2}}\left(f^{(l)}(x)\right)^2 dx\right| &= \left|\sum_{l=2}^{r-1}\left(\frac{h_i + h_{i-1}}{2}\right)^{2l-1}\int_{x_{i-1/2}}^{x_{i+1/2}}\left(((p^{r-1}_{i,n}(x))^{(l)})^2 - \left(f^{(l)}(x)\right)^2\right) dx\right| \\ &\leq \sum_{l=2}^{r-1}\left(\frac{h_i + h_{i-1}}{2}\right)^{2l-1}\int_{x_{i-1/2}}^{x_{i+1/2}}\left|((p^{r-1}_{i,n}(x))^{(l)})^2 - \left(f^{(l)}(x)\right)^2\right| dx \\ &\leq \sum_{l=2}^{r-1}\left(\frac{h_i + h_{i-1}}{2}\right)^{2l} O(h^{r-l}) \\ &\leq O(h^{r+3}). \end{aligned} \tag{26}$$

Thus, we obtain:

$$\begin{aligned} \left|I^{r-1}_{i,k} - I^{r-1}_{i,k_1}\right| \leq& \left|I^{r-1}_{i,k} - \sum_{l=2}^{r-1}\left(\frac{h_i + h_{i-1}}{2}\right)^{2l-1}\int_{x_{i-1/2}}^{x_{i+1/2}}\left(f^{(l)}(x)\right)^2 dx\right| \\ &+ \left|I^{r-1}_{i,k_1} - \sum_{l=2}^{r-1}\left(\frac{h_i + h_{i-1}}{2}\right)^{2l-1}\int_{x_{i-1/2}}^{x_{i+1/2}}\left(f^{(l)}(x)\right)^2 dx\right| \\ =& O(h^{r+3}). \end{aligned} \tag{27}$$

■

Lemma 4.3. *Let $0 \leq k, k_1 \leq r-1$, $1 \leq \theta$ and let I^{r-1}_n, $n = k, k_1$ be smoothness indicators of f on the stencil $\mathcal{S}^r_{i,n} = \{x_{i-(r-1)+n}, \cdots, x_{i+n}\}$ and p^{r-1}_{i,k_1} be the interpolating polynomial of f at nodes in the stencil $\mathcal{S}^r_{k_1}$. If $f \in C^r([x_{i+n-(r-1)}, x_{i+n}])$ and $\epsilon = O(h^4)$ or $I^{r-1}_{i,k_1} = O(h^4)$ then:*

$$\frac{I^{r-1}_{i,k} - I^{r-1}_{i,k_1}}{\epsilon - I^{r-1}_{i,k_1}} = O(h^{r-1}), \tag{28}$$

and

$$\frac{1}{(\epsilon - I^{r-1}_{i,k})^\theta} = \frac{1 + O(h^{r-1})}{(\epsilon - I^{r-1}_{i,k_1})^\theta}. \tag{29}$$

Proof. The proof of Eq. (28) is direct by Lemmas 4.1 and 4.2. In order to proof Eq. (29), we use the following algebraic manipulation (see [6]):

$$\frac{1}{(\epsilon + I^{r-1}_{i,k})^\theta} = \frac{1}{(\epsilon + I^{r-1}_{i,k_1})^\theta} + \frac{1}{(\epsilon + I^{r-1}_{i,k_1})^\theta}\left(\frac{I^{r-1}_{i,k_1} - I^{r-1}_{i,k}}{\epsilon + I^{r-1}_{i,k}}\sum_{j=0}^{\theta-1}\left(\frac{\epsilon + I^{r-1}_{i,k_1}}{\epsilon + I^{r-1}_{i,k}}\right)^j\right).$$

■

Notice that if $I^{r-1}_{i,k_1} = O(h^m)$ with $m > 4$ and $0 < \epsilon < h^m$ is a fixed value, then Lemma 4.3 is not satisfied and the optimal order is not obtained. This is explained in detail in [6]. In all our experiments, as we have mentioned in Section 1, we have set $\epsilon = 10^{-16}$. This way, the order of accuracy of the smoothness indicators will be $O(h^4)$ at the smooth parts of the data. In the rest of the paper, we always consider these conditions.

Proposition 4.4. *Let $0 \leq k \leq r-1$, $1 \leq \theta$ and $\omega_{i,k}^{r-1}$ the nonlinear weights defined in Eq.* (10)*, then*

$$\omega_{i,k}^{r-1} = O(1), \quad \text{if } f \text{ is smooth in } \mathcal{S}_{i,k}^r,$$
$$\omega_{i,k}^{r-1} = O(h^{2m\theta}), \quad \text{if } f \text{ is not smooth in } \mathcal{S}_{i,k}^r.$$

with $m = 2$ if the discontinuity is in the function and $m = 1$ if the discontinuity is in the first derivative.

Also, if f is smooth in $\{x_{i-(r-1)}, \dots, x_{i+(r-1)}\}$ then:

$$\omega_{i,k}^{r-1} = C_{i,k}^{r-1} + O(h^{r-1}),$$

being $C_{i,k}^{r-1}$ the optimal weights defined in Eq. (1.1)*.*

Proof. Let be $0 \leq k, n < r-1$. If f is smooth in $\mathcal{S}_n^r$ then using (10) and Lemma 4.1:

$$\alpha_{i,n}^{r-1} = \frac{C_{i,n}^{r-1}}{(\epsilon + I_{i,n}^{r-1})^\theta} = O(h^{-4\theta}) \to \sum_{l=0}^{r-1} \alpha_{i,l}^{r-1} = O(h^{-4\theta}),$$

then it is clear that, if f is smooth in $\mathcal{S}_{i,k}^r$:

$$\omega_{i,k}^{r-1} = \frac{\alpha_{i,k}^{r-1}}{\sum_{l=0}^{r-1} \alpha_{i,l}^{r-1}} = O(1),$$

and if f is not smooth in $\mathcal{S}_{i,k}^r$:

$$\omega_{i,k}^{r-1} = \frac{\alpha_{i,k}^{r-1}}{\sum_{l=0}^{r-1} \alpha_{i,l}^{r-1}} = O(h^{2m\theta}),$$

being $m = 2$ is the discontinuity is in the function and $m = 1$ is the discontinuity is in the first derivative. Finally, if f is smooth in $\{x_{i-(r-1)}, \dots, x_{i+(r-1)}\}$, we fix a value $0 \leq k_1 \leq r-1$ and using (29) in Lemma 4.3, we get for all $0 \leq k \leq r-1$:

$$\alpha_{i,k}^{r-1} = \frac{C_{i,k}^{r-1}}{(\epsilon + I_{i,k}^{r-1})^\theta} = \frac{C_{i,k}^{r-1}(1 + O(h^{r-1}))}{(\epsilon + I_{i,k_1}^{r-1})^\theta} \to \sum_{l=0}^{r-1} \alpha_{i,l}^{r-1} = \frac{1 + O(h^{r-1})}{(\epsilon + I_{i,k_1}^{r-1})^\theta}.$$

Therefore,

$$\omega_{i,k}^{r-1} = \frac{\alpha_{i,k}^{r-1}}{\sum_{l=0}^{r-1} \alpha_{i,l}^{r-1}} = \frac{\frac{C_{i,k}^{r-1}(1+O(h^{r-1}))}{(\epsilon+I_{i,k_1}^{r-1})^\theta}}{\frac{1+O(h^{r-1})}{(\epsilon+I_{i,k_1}^{r-1})^\theta}} = \frac{C_{i,k}^{r-1}(1 + O(h^{r-1}))}{1 + O(h^{r-1})} = C_{i,k}^{r-1}(1 + O(h^{r-1})).$$

■

In order to construct the smoothness indicators for each "level", we consider where the discontinuities are placed. In order to clarify the explanation we start with an example, for $r = 4$. In Sec. 2.2 we have seen that we should define I_{i,k,k_1}^l with $l = 4, 5$, $k = 0, 1$, $k_1 = k, k+1$, then we have the following scheme:

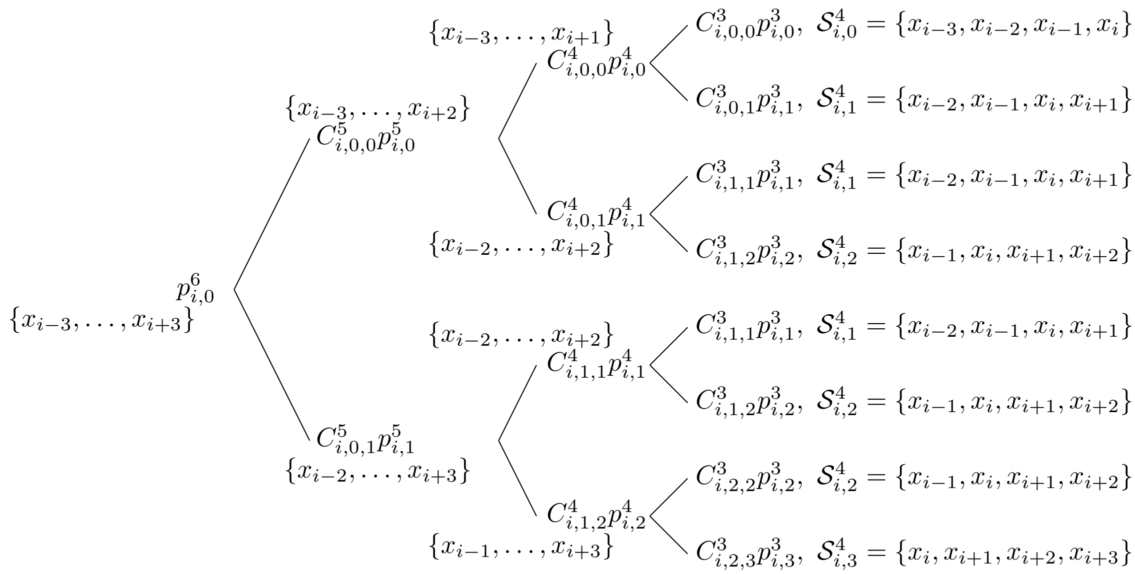

Figure 1: Diagram showing the structure of the optimal weights needed to obtain optimal order of accuracy for $r = 4$.

We suppose that the discontinuities are far enough from each other, i.e., there only exists one discontinuity at an interval. Thus, we have the following cases:

- There does not exist any discontinuity: We use all the weights.
- There exists a discontinuity at (x_{i+2}, x_{i+3}): In this case, the points that are used to construct the interpolator are $\{x_{i-3}, \dots, x_{i+2}\}$. Therefore, we have to obtain $\omega^5_{0,0} = O(1)$, $\omega^5_{0,1} = O(h^2)$, $\omega^4_{0,0} = O(1)$ and $\omega^4_{0,1} = O(1)$ (the rest of the weights are not important because $\omega^5_{0,1} = O(h^2)$). Notice that using the scheme in Fig. 2, we are choosing $I^6_{i,0,0} = I^3_{i,0,0}$ and we get the desired result.

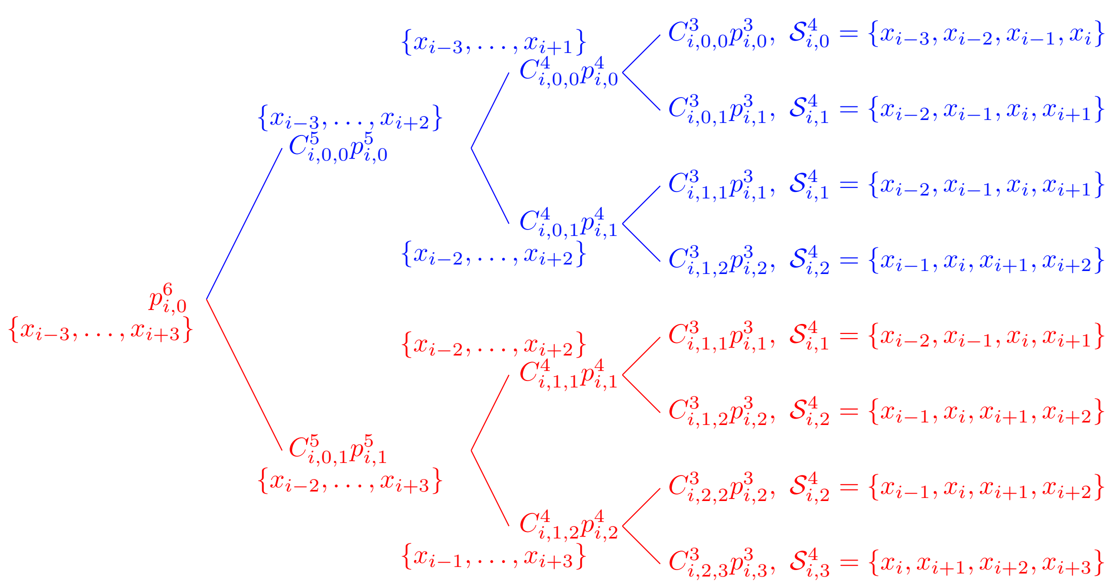

Figure 2: First case: discontinuity at (x_{i+2}, x_{i+3}). Red: polynomials that are not used. Blue: polynomials that are used.

- There exists a discontinuity at (x_{i+1}, x_{i+2}): The largest stencil not contaminated by the discontinuity is

$\{x_{i-3},\dots,x_{i+1}\}$. Therefore, we have to obtain $\omega^5_{0,1}=O(h^2)$ and $\omega^5_{0,0}=O(1)$, $\omega^4_{0,0}=O(1)$ and $\omega^4_{0,1}=O(1)$. In Fig. 3 we write in red the branch that is not used because a discontinuity is contained in the stencil. In green, the stencil that is used although it contains a discontinuity and in blue, the stencils which do not contain any discontinuity. Therefore, we define $I^6_{i,0,0}=I^3_{i,0,0}$ and $I^5_{i,1,1}=I^3_{i,1,1}$.

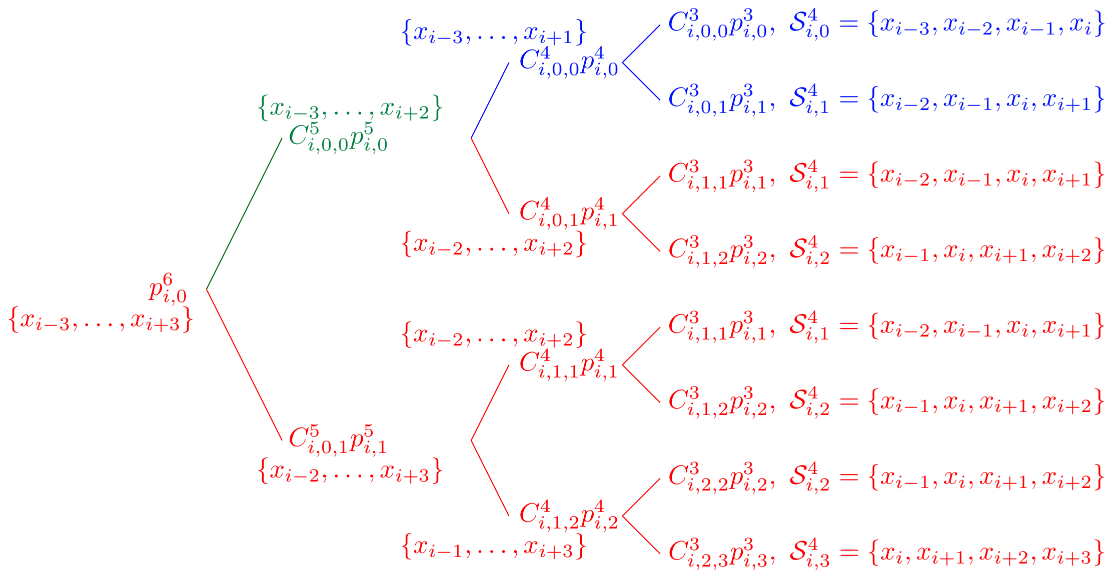

Figure 3: Second case: discontinuity at (x_{i+1},x_{i+2}). Red: polynomials that are not used. Blue: polynomials used. Green: polynomial affected by a discontinuity but not eliminated branch.

- There exists a discontinuity at (x_i,x_{i+1}): The largest stencil that does not contain a discontinuity is $\mathcal{S}^4_{i,0}=\{x_{i-3},\dots,x_i\}$. In this case, only the classical WENO interpolator can be recovered.

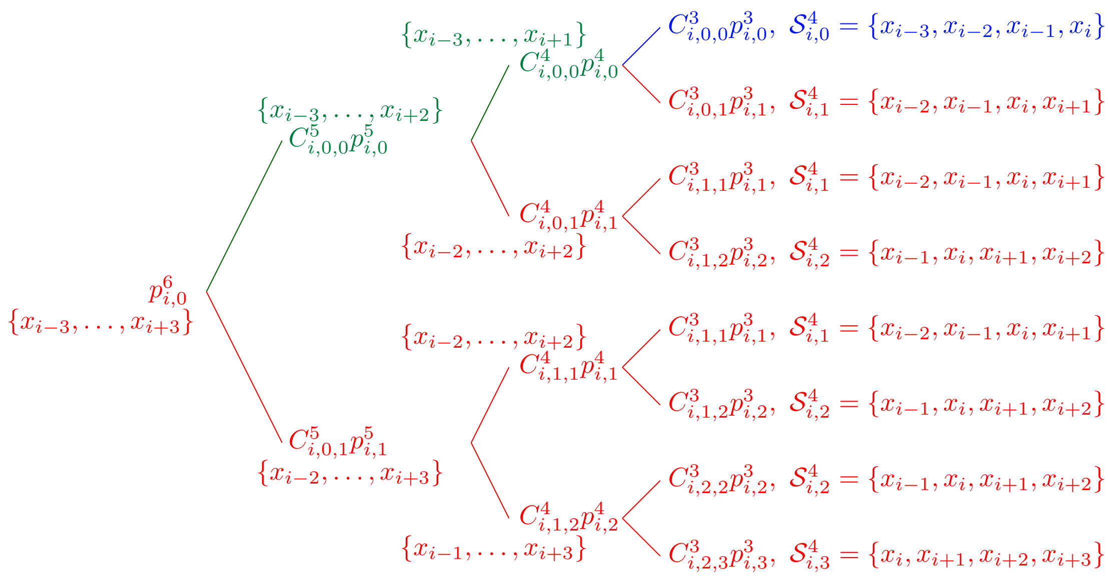

Figure 4: Third case: discontinuity at (x_i,x_{i+1}). Red: polynomials that are not used. Blue: polynomials used. Green: polynomial affected by a discontinuity but not-eliminated branch.

- The rest of the cases are symmetric.

Hence, if $I_{i,k}^{r-1}$, $k=0,\dots,3$ are the smoothness indicators defined in Eq. (11) for $r=4$ then:

$$I_{i,0,0}^5=I_{i,0}^3,\ I_{i,0,1}^5=I_{i,3}^3,\ I_{i,0,0}^4=I_{i,0}^3,\ I_{i,0,1}^4=I_{i,2}^3,\ I_{i,1,1}^4=I_{i,1}^3,\ I_{i,1,2}^4=I_{i,3}^3. \tag{30}$$

Using this example, we introduce the following definition.

Definition 1. *General smoothness indicators.*

Let $I_{i,k}^{r-1}$, with $k=0,\dots,r-1$ be the smoothness indicators shown in Eq. (11), then we define the smoothness indicators for any r as:

$$\begin{aligned} I_{i,k,k}^l &= I_{i,k}^{r-1}, \quad k=0,\dots,(2r-3)-l,\\ I_{i,k,k+1}^l &= I_{i,l+k+2-r}^{r-1}, \quad k=0,\dots,(2r-3)-l. \end{aligned} \tag{31}$$

with $r\le l\le 2r-3$.

The following lemma is similar to Prop. 4.4 for nonlinear weights at each level.

Lemma 4.5. *Let $r\le l\le 2r-3$, $0\le k\le(2r-3)-l$, $1\le\theta$ and let ω_{i,k,k_1}^l, with $k_1=k,k+1$ be the nonlinear weights defined in Eq. (22) then*

1. *If neither $I_{i,k,k}^l$ and $I_{i,k,k+1}^l$ are affected by a discontinuity, then $\omega_{i,k,k}^l=C_{i,k,k}^l(1+O(h^{r-1}))$, $\omega_{i,k,k+1}^l=C_{i,k,k+1}^l(1+O(h^{r-1}))$.*
2. *If $I_{i,k,k+1}^l$ is affected by a singularity then $\omega_{i,k,k}^l=1+O(h^{2m\theta})$, $\omega_{i,k,k+1}^l=O(h^{2m\theta})$.*
3. *If $I_{i,k,k}^l$ is affected by a singularity then $\omega_{i,k,k}^l=O(h^{2m\theta})$, $\omega_{i,k,k+1}^l=1+O(h^{2m\theta})$.*

Here, $m=2$ if the discontinuity is in the function and $m=1$ if the discontinuity is in the first derivative

Proof. It is similar to Prop. 4.4: From $C_{i,k,k}^l+C_{i,k,k+1}^l=1$, using the definition given in (22), we have that:

1. If $I_{i,k,k}^l=O(h^4)$ and $I_{i,k,k+1}^l=O(h^4)$, by Eq. (29) in Lemma 4.3, we get:

$$\begin{aligned} \alpha_{i,k,k}^l &= \frac{C_{i,k,k}^l}{(\epsilon+I_{i,k,k}^l)^\theta}=\frac{C_{i,k,k}^l(1+O(h^{r-1}))}{(\epsilon+I_{i,k,k+1}^l)^\theta},\\ \omega_{i,k,k}^l &= \frac{\alpha_{i,k,k}^l}{\alpha_{i,k,k}^l+\alpha_{i,k,k+1}^l}=\frac{\frac{C_{i,k,k}^l(1+O(h^{r-1}))}{(\epsilon+I_{i,k,k+1}^l)^\theta}}{\frac{C_{i,k,k}^l(1+O(h^{r-1}))}{(\epsilon+I_{i,k,k+1}^l)^\theta}+\frac{C_{i,k,k+1}^l}{(\epsilon+I_{i,k,k+1}^l)^\theta}}=\frac{C_{i,k,k}^l(1+O(h^{r-1}))}{C_{i,k,k}^l(1+O(h^{r-1}))+C_{i,k,k+1}^l}\\ &= C_{i,k,k}^l(1+O(h^{r-1})). \end{aligned}$$

   Analogously for $\omega_{i,k,k+1}^l$.

2. If $I_{i,k,k}^l=O(h^4)$ and $I_{i,k,k+1}^l=O(1)$ if the discontinuity is in the function or $I_{i,k,k+1}^l=O(h^2)$ if the discontinuity is in the first derivative:

$$\begin{aligned} \omega_{i,k,k}^l &= \frac{C_{i,k,k}^l(\epsilon+I_{i,k,k+1}^l)^\theta}{C_{i,k,k}^l(\epsilon+I_{i,k,k+1}^l)^\theta+C_{i,k,k+1}^l(\epsilon+I_{i,k,k}^l)^\theta}\\ &= \frac{C_{k,k}^l(\epsilon+I_{i,k,k+1}^l)^\theta}{C_{i,k,k}^l(\epsilon+I_{i,k,k+1}^l)^\theta+O(h^{4\theta})}=\frac{C_{i,k,k}^l(\epsilon+I_{i,k,k+1}^l)^\theta}{C_{i,k,k}^l(\epsilon+I_{i,k,k+1}^l)^\theta}\frac{1}{1+\frac{O(h^{4\theta})}{C_{i,k,k}^l(\epsilon+I_{i,k,k+1}^l)^\theta}}\\ &= 1+O(h^{2m\theta}),\\ \omega_{i,k,k+1}^l &= \frac{C_{i,k,k+1}^l(\epsilon+I_{i,k,k}^l)^\theta}{C_{i,k,k}^l(\epsilon+I_{i,k,k+1}^l)^\theta+C_{i,k,k+1}^l(\epsilon+I_{i,k,k}^l)^\theta}=\frac{O(h^{4\theta})}{O(h^{\tilde m\theta})+O(h^{4\theta})}=O(h^{(4-\tilde m)\theta}),\ \tilde m=0,2. \end{aligned} \tag{32}$$

3. Analogously if $I_{i,k,k}^l=O(1)$ and $I_{i,k,k+1}^l=O(h^{2m})$.

■

If we analyse the examples presented, we can determine a rule for the weights and try to prove it. In the first case, Fig. 2, the discontinuity is in the interval $(x_{i+(l_0-1)}, x_{i+(l_0-1)}) = (x_{i+2}, x_{i+3})$, (i.e. $l_0 = 3$), and we can see that the branch marked in red is the one corresponding to $p^5_{i,1}$, thus $\omega^l_{i,0,1} = \omega^{(r-2)+l_0}_{i,0,1} = \omega^5_{i,0,1}$ should be $O(h^2)$. In the second case, Fig. 3, the discontinuity is in the interval (x_{i+1}, x_{i+2}), $(l_0 = 2)$, and the red branches are in the corresponding to $p^4_{i,1}$, then $\omega^{(r-2)+l_0}_{i,0,1} = \omega^4_{i,0,1}$ and $\omega^5_{i,0,1}$ should be $O(h^2)$. We prove that the weights of the different branches which contain a discontinuity go to 0 as $h \to 0$, in the following lemma.

Lemma 4.6. *Let $2 \leq l_0 \leq r-1$. If f is smooth in $[x_{i-(r-1)}, x_{i+(r-1)}] \setminus (x_{i+(l_0-1)}, x_{i+l_0})$, then for all $(r-2)+l_0 \leq l \leq 2r-3$ the nonlinear weights defined in Eq. (22) satisfy:*

$$\omega^l_{i,0,0} = 1 + O(h^{2m\theta}),\ \omega^l_{i,0,1} = O(h^{2m\theta}).$$

with $m = 2$ if the discontinuity is in the function and $m = 1$ if the discontinuity is in the first derivative.

Proof. Let $2 \leq l_0 \leq r-1$ and $(r-2)+l_0 \leq l \leq 2r-3$. If the discontinuity is in $(x_{i+(l_0-1)}, x_{i+l_0})$ then $I^{r-1}_{i,0} = O(h^4)$ since $\mathcal{S}^r_0 = \{x_{i-(r-1)}, \dots, x_i\}$ and $l_0 \geq 1$. Subsequently, the stencil used to calculate $I^{r-1}_{i,l+2-r}$ is $\mathcal{S}^r_{l+2-r} = \{x_{i-(r-1)+l+2-r}, \dots, x_{i+l+2-r}\}$, as $(r-2)+l_0 \leq l \leq 2r-3$ then $l_0 \leq l+2-r$, therefore $I^{r-1}_{i,l+2-r} = O(1)$ if the discontinuity is in the function or $I^{r-1}_{i,l+2-r} = O(h^2)$ if the function contains a kink discontinuity. By Def. 1 we have that $I^l_{i,0,1} = I^{r-1}_{i,l+2-r} = O(h^{\tilde{m}})$, $\tilde{m} = 0, 2$. Using Lemma 4.5 we finish the proof. ■

Lemma 4.7. *Let $2 \leq l_0 \leq r-1$. If f is smooth in $[x_{i-(r-1)}, x_{i+(r-1)}] \setminus (x_{i+(l_0-1)}, x_{i+l_0})$, then for all $r \leq l \leq l_0 + (r-2) - 1$ the nonlinear weights defined in Eq. (22) satisfy:*

$$\omega^l_{i,k,k} = C^l_{i,k,k} + O(h^{r-1}), \quad \omega^l_{i,k,k+1} = C^l_{i,k,k+1} + O(h^{r-1}), \quad 0 \leq k \leq l_0 + (r-2) - 1 - l, \tag{33}$$

being C^l_{i,k,k_1} with $k_1 = k,\ k+1$ defined in Eq. (16).

Proof. Let $2 \leq l_0 \leq r-1$ and $r \leq l \leq l_0 + (r-2) - 1$. We analyse the stencils used to calculate $I^l_{i,k,k}$ and $I^l_{i,k,k+1}$ with $0 \leq k \leq l_0 + (r-2) - 1 - l$. First of all, we take into account two previous considerations:

From $r \leq l$, we get:

$$0 \leq k \leq l_0 + (r-2) - 1 - l \leq l_0 + (r-2) - 1 - r = l_0 - 3, \tag{34}$$

and from $k \leq l_0 + (r-2) - 1 - l$:

$$l + k + 2 - r \leq l + l_0 + (r-2) - 1 - l + 2 - r = l_0 - 1. \tag{35}$$

By Def. 1 we have that:

1. $I^l_{i,k,k} = I^{r-1}_{i,k}$, then the stencil used is $\mathcal{S}^r_{i,k} = \{x_{i-(r-1)+k}, \dots, x_{i+k}\}$. Using (34), the stencil does not cross the discontinuity and $I^l_{i,k,k} = I^{r-1}_{i,k} = O(h^4)$
2. $I^l_{i,k,k+1} = I^{r-1}_{i,l+k+2-r}$, then the stencil used is $\mathcal{S}^r_{i,l+k+2-r} = \{x_{i-(r-1)+l+k+2-r}, \dots, x_{i+l+k+2-r}\}$. Using (34), analogously, $I^l_{i,k,k+1} = I^{r-1}_{i,l+k+2-r} = O(h^4)$.

By Lemma 4.5 we get the result. ■

With the ingredients presented in the previous sections we can prove the following lemma. We suppose that the isolated discontinuity is to the right of the point x_i. By symmetry, the analysis for the left side would be similar.

Lemma 4.8. *Let $2 \leq l_0 \leq r-1$. If f is smooth in $[x_{i-(r-1)}, x_{i+(r-1)}] \setminus (x_{i+(l_0-1)}, x_{i+l_0})$, then the nonlinear weights $\tilde{\omega}^{r-1}_{i,k}$, $k = 0, \dots, r-1$ defined in Eq. (24) satisfy:*

$$(\tilde{\omega}^{r-1}_{i,0}, \tilde{\omega}^{r-1}_{i,1}, \dots, \tilde{\omega}^{r-1}_{i,r-1}) = (\hat{C}^{r-1}_{i,0} + O(h^{r-1}), \hat{C}^{r-1}_{i,1} + O(h^{r-1}), \dots, \hat{C}^{r-1}_{i,l_0-1} + O(h^{r-1}), O(h^{2m\theta}), \dots, O(h^{2m\theta})), \tag{36}$$

with $m = 2$ if the discontinuity is in the function and $m = 1$ if the discontinuity is in the first derivative, being

$$\frac{dp^{r+l_0-2}_{i,0}}{dx}(x_i) = \sum_{k=0}^{l_0-1} \hat{C}^{r-1}_{i,k} \frac{dp^{r-1}_{i,k}}{dx}(x_i).$$

Proof. Applying Eq. (19) to the interpolatory polynomial $p_{i,0}^{r+l_0-2}$ and Lemmas 4.6 and 4.7, we obtain that:

$$(\omega_{i,0}^{r-1},\omega_{i,1}^{r-1},\dots,\omega_{i,r-1}^{r-1}) = (\hat{C}_{i,0}^{r-1}+O(h^{r-1}),\hat{C}_{i,1}^{r-1}+O(h^{r-1}),\dots,\hat{C}_{i,l_0-1}^{r-1}+O(h^{r-1}),O(h^{2m\theta}),\dots,O(h^{2m\theta})), \quad (37)$$

with $m=2$ if the discontinuity is in the function and $m=1$ if the discontinuity is in the first derivative, being

$$\frac{dp_{i,0}^{r+l_0-2}}{dx}(x_i) = \sum_{k=0}^{l_0-1}\hat{C}_{i,k}^{r-1}\frac{dp_{i,k}^{r-1}}{dx}(x_i).$$

As $\sum_{k=0}^{l_0-1}\hat{C}_{i,k}^{r-1}=1$ we get the result. ■

Using Lemma 4.8, it is easy to prove the main result. We obtain a progressive order of approximation for the derivative values close to the discontinuities.

Theorem 4.9. *Let $1\le l_0\le r-1$ and let $\tilde{\omega}_{i,k}^{r-1}$ be defined in Eq. (24) with $\theta\ge r-1$. If f is smooth in $[x_{i-(r-1)},x_{i+(r-1)}]\setminus\Omega$ and f has a discontinuity at Ω then*

$$\sum_{k=0}^{r-1}\tilde{\omega}_k^{r-1}\frac{dp_{i,k}^{r-1}}{dx}(x_i)-\frac{df}{dx}(x_i) = \begin{cases} O(h^{2r-2}), & \text{if } \Omega=\emptyset; \\ O(h^{(r-2)+l_0}), & \text{if } \Omega=(x_{i+(l_0-1)},x_{i+l_0}). \end{cases} \quad (38)$$

Also, if $l_0>r-1$ then:

$$\sum_{k=0}^{r-1}\tilde{\omega}_k^{r-1}\frac{dp_{i,k}^{r-1}}{dx}(x_i)-\frac{df}{dx}(x_i) = O(h^{2r-2}). \quad (39)$$

Proof. If f is smooth in the stencil $\{x_{i-(r-1)+k},\dots,x_{i-(r-1)+k+l}\}$ then $\frac{df}{dx}(x_i)-\frac{dp_{i,k}^{l}}{dx}(x_i)=O(h^l)$. Let $2\le l_0\le r-1$, then

$$\begin{aligned}
\sum_{k=0}^{r-1}\tilde{\omega}_{i,k}^{r-1}\frac{dp_{i,k}^{r-1}}{dx}(x_i)-\frac{df}{dx}(x_i) &= \sum_{k=0}^{r-1}\tilde{\omega}_{i,k}^{r-1}\frac{dp_{i,k}^{r-1}(x_i)}{dx}-\frac{dp_{i,0}^{l_0+r-2}}{dx}(x_i)+\frac{dp_{i,0}^{l_0+r-2}}{dx}(x_i)-\frac{df}{dx}(x_i)\\
&= \sum_{k=0}^{r-1}(\tilde{\omega}_{i,k}^{r-1}-\hat{C}_{i,k}^{r-1})\frac{dp_{i,k}^{r-1}}{dx}(x_i)+O(h^{r+l_0-2})\\
&= \sum_{k=0}^{l_0-1}(\tilde{\omega}_k^{r-1}-\hat{C}_{i,k}^{r-1})\left(\frac{dp_{i,k}^{r-1}}{dx}(x_i)-\frac{df}{dx}(x_i)\right)+\sum_{k=l_0}^{r-1}\tilde{\omega}_{i,k}^{r-1}\left(\frac{dp_{i,k}^{r-1}}{dx}(x_i)-\frac{df}{dx}(x_i)\right)+O(h^{r+l_0-2})\\
&= O(h^{r-1+r-1})+O(h^{2m\theta})+O(h^{r+l_0-2}) = O(h^{r+l_0-2}).
\end{aligned}$$

■

Therefore, we have proved that, when the isolated discontinuities affect the stencil, we get maximal order in a neighbourhood of the interval where it is located. In the next section we show some experiments that confirm this theoretical result.

5. Numerical experiments and conclusions

In this section we present some numerical experiments in order to verify the theoretical results shown in previous sections. We will use the following function:

$$f_\eta(x) = \begin{cases} x^{10}-x^9+x^8-4x^7+x^6+x^5+x^4+x^3+5x^2+3x, & x<0,\\ \eta-(x^{10}-2x^9+3x^8-8x^7-2x^6+x^5-2x^4-3x^3-5x^2+3x), & x\ge 0, \end{cases} \quad (40)$$

discretized in the interval $[-\frac{\pi}{6},1-\frac{\pi}{6}]$ using $J_q=2^q+1$ uniform spaced points where $\eta=0,10$. In the first case, the function f_0 is continuous but it presents a discontinuity in the first derivative and in the second case, f_{10} has a jump discontinuity. We denote the interval where the discontinuity is contained as (x_{i-1},x_i) and we compute the error as

$$e_{l_0}^q = \left|\frac{d}{dx}f(x_{i+l_0})-ap(x_{i+l_0})\right|, \quad (41)$$

being ap the approximation of the derivative values using the following methods:

- [lin-($2r-2$)] Linear Lagrange method using a centered stencil of $2r-1$ points.
- [WENO-($2r-2$)] Non-linear using the classical WENO algorithm explained in Section 1, Eq. (3).
- [p-WENO-($2r-2$)] New progressive order WENO algorithm introduced in this work.

Finally, we compute the numerical order of accuracy using the formula:

$$o_{l_0}^q = \frac{e_{l_0}^q}{e_{l_0}^{q+1}}. \tag{42}$$

We start using a large stencil of 5 points, i.e. $r=3$, and, using the linear method, we expect to obtain four consecutive points where the order is lost. Using classical WENO method, we will typically obtain order 3 at the points where the order is lost using the linear method. Using the new algorithm we expect to obtain progressive order of accuracy $(r-1, r, 2r-2) = (2, 3, 4)$. We show the results for $r=3$ in Tables 4, 5 and 6 for f_0 and 10, 11 and 12 for f_{10}. For $r=4$, we can see the results in Tables 7, 8 and 9 for the first experiment and 13, 14 and 15 for the second one. It is clear that the new algorithm produces better approximation close to the discontinuity. We obtain the same results to the left of the discontinuity. Finally, it is important to remark that if the function is continuous but it presents a discontinuity in the first derivative, i.e. a kink, we can not use the smoothness indicators introduced in Eq. (11).

6. Conclusions

In this work a new WENO algorithm with progressive order of accuracy close to discontinuities has been introduced. It allows to calculate approximations of derivative values of a function using regular or non-regular grids. It is based on the same ideas used in [3] which consist in using Aitken process to calculate the nonlinear weights. The explicit formulas for the optimal weights have been showed and the order of accuracy in each interval has been proved. Finally, some experiments have been presented that confirm the theoretical results obtained.

References

[1] M. Abramowitz, and I. A. Stegun, (2010): Handbook of Mathematical Functions with Formulas, Graphs, and Mathematical Tables, Cambridge University Press, Dover, New York.

[2] S. Amat, J. Ruiz (2017): "New WENO smoothness indicators computationally efficient in presence of corner discontinuities', *J. Sci. Comput. 71*, 1265-1237.

[3] S. Amat, J. Ruiz, C.W. Shu, D. F. Yáñez, (2020): "A new WENO-$2r$ Algorithm with progressive order of accuracy close to discontinuities", *SIAM J. Numer. Anal., 58(6)*, 3448-3474.

[4] S. Amat, J. Ruiz, C.W. Shu, D. F. Yáñez, (2021): "Cell-average WENO with progressive order of accuracy close to discontinuities with applications to signal processing", *Appl. Math. Comput. 403*, 126131.

[5] F. Aràndiga, A. Baeza, A. M. Belda, P. Mulet, (2011): "Analysis of WENO schemes for full and Global accuracy", *SIAM J. Numer. Anal., 49(2)*, 893-915.

[6] F. Aràndiga, A. M. Belda, P. Mulet, (2010): "Point-Value WENO Multiresolution Applications to Stable Image Compression", *J. Sci. Comput. 43(2)*, 158-182.

[7] G. Jiang and D. Peng, (2000): "Weighted ENO schemes for Hamilton-Jacobi equations", *SIAM J. Sci. Comput., 21*, 2126-2143.

[8] G. Jiang and C.-W. Shu, (1996): "Efficient Implementation of Weighted ENO Schemes", *J. Comput. Phys., 126(1)*, 202-228.

[9] D. Levy, G. Puppo and G. Russo, (1999): "Central WENO schemes for hyperbolic systems of conservation laws", *Mathematical Modelling and Numerical Analysis, 33(3)*, 547-571.

[10] X.-D. Liu and S. Osher and T. Chan, (1994): "Weighted Essentially Non-oscillatory Schemes", *J. Comput. Phys., 115*, 200-212.

[11] C.-W. Shu, (1999): “High Order Weighted Essentially Nonoscillatory Schemes for Convection Dominated Problems”, *SIAM Review, 51(1)*, 82–126.

[12] D. F. Yáñez, (2010): “Learning Multiresolution: transformaciones multiescala derivadas de la teoría de aprendizaje y aplicaciones.”, PhD. Thesis, Valencia, 2010.

q	e_1^q	o_1^q	e_2^q	o_2^q	e_3^q	o_3^q	e_4^q	o_4^q	e_5^q	o_5^q	e_6^q	o_6^q
5	$2.1434e+00$	-	$3.7751e-01$	-	$3.8405e-06$	-	$2.9591e-06$	-	$1.5404e-06$	-	$3.9272e-07$	-
6	$1.2862e+00$	0.74	$2.5516e-01$	0.57	$2.6340e-07$	3.87	$2.5774e-07$	3.52	$2.4316e-07$	2.66	$2.1983e-07$	0.84
7	$4.2774e-01$	1.59	$1.0322e-02$	4.63	$1.6297e-08$	4.01	$1.6477e-08$	3.97	$1.6513e-08$	3.88	$1.6406e-08$	3.74
8	$3.5549e-01$	0.27	$2.0643e-02$	-1.00	$9.8526e-10$	4.05	$9.9893e-10$	4.04	$1.0103e-09$	4.03	$1.0194e-09$	4.01
9	$2.1099e-01$	0.75	$4.1287e-02$	-1.00	$6.0034e-11$	4.04	$6.0590e-11$	4.04	$6.1111e-11$	4.05	$6.1589e-11$	4.05

Table 4: Grid refinement analysis for the linear Lagrange method for $r = 3$ algorithm for the function in (40) for f_0, i.e. $\eta = 0$.

q	e_1^q	o_1^q	e_2^q	o_2^q	e_3^q	o_3^q	e_4^q	o_4^q	e_5^q	o_5^q	e_6^q	o_6^q
5	$2.2231e-03$	-	$5.1191e-04$	-	$4.9491e-06$	-	$4.7419e-06$	-	$2.6510e-06$	-	$2.1599e-06$	-
6	$5.2818e-04$	2.07	$1.1285e-04$	2.18	$2.6489e-07$	4.22	$2.9352e-07$	4.01	$3.1452e-07$	3.08	$3.2063e-07$	2.75
7	$2.6023e-04$	1.02	$3.3248e-05$	1.76	$1.4689e-08$	4.17	$1.5617e-08$	4.23	$1.6576e-08$	4.25	$1.7520e-08$	4.19
8	$3.1408e-05$	3.05	$6.3688e-06$	2.38	$8.4033e-10$	4.13	$8.6444e-10$	4.18	$8.9040e-10$	4.22	$9.1788e-10$	4.25
9	$7.7296e-06$	2.02	$1.5575e-06$	2.03	$5.0505e-11$	4.06	$5.1136e-11$	4.08	$5.1804e-11$	4.10	$5.2511e-11$	4.13

Table 5: Grid refinement analysis for the classical WENO method for $r = 3$ algorithm for the function in (40) for f_0, i.e. $\eta = 0$.

q	e_1^q	o_1^q	e_2^q	o_2^q	e_3^q	o_3^q	e_4^q	o_4^q	e_5^q	o_5^q	e_6^q	o_6^q
5	$2.2187e-03$	-	$6.5048e-05$	-	$1.0293e-05$	-	$1.8900e-05$	-	$3.2851e-05$	-	$5.3130e-05$	-
6	$5.2818e-04$	2.07	$6.3719e-06$	3.35	$3.4382e-07$	4.90	$4.7387e-07$	5.32	$6.5198e-07$	5.65	$8.9250e-07$	5.90
7	$1.9464e-04$	1.44	$7.3526e-07$	3.12	$1.5543e-08$	4.47	$1.8318e-08$	4.69	$2.1531e-08$	4.92	$2.5284e-08$	5.14
8	$3.1377e-05$	2.63	$7.9347e-08$	3.21	$7.4984e-10$	4.37	$8.1986e-10$	4.48	$8.9371e-10$	4.59	$9.7210e-10$	4.70
9	$7.7296e-06$	2.02	$9.4094e-09$	3.08	$4.0669e-11$	4.20	$4.2700e-11$	4.26	$4.4769e-11$	4.32	$4.6879e-11$	4.37

Table 6: Grid refinement analysis for the new WENO method for $r = 3$ algorithm for the function in (40) for f_0, i.e. $\eta = 0$.

q	e_1^q	o_1^q	e_2^q	o_2^q	e_3^q	o_3^q	e_4^q	o_4^q	e_5^q	o_5^q	e_6^q	o_6^q
5	$2.0944e+00$	-	$5.0417e-01$	-	$7.5502e-02$	-	$1.1512e-07$	-	$1.1023e-07$	-	$1.0457e-07$	-
6	$1.1883e+00$	0.82	$3.0828e-01$	0.71	$5.1031e-02$	0.57	$1.9137e-09$	5.91	$1.8731e-09$	5.88	$1.8353e-09$	5.83
7	$6.2362e-01$	0.93	$8.3483e-02$	1.88	$2.0643e-03$	4.63	$3.0962e-11$	5.95	$3.0591e-11$	5.94	$3.0230e-11$	5.92
8	$5.4724e-01$	0.19	$6.6970e-02$	0.32	$4.1287e-03$	-1.00	$4.9560e-13$	5.97	$4.9072e-13$	5.96	$4.8894e-13$	5.95
9	$3.9448e-01$	0.47	$3.3941e-02$	0.98	$8.2573e-03$	-1.00	$7.1054e-15$	6.12	$1.1990e-14$	5.35	$7.5495e-15$	6.02

Table 7: Grid refinement analysis for the linear Lagrange method for $r = 4$ algorithm for the function in (40) for f_0, i.e. $\eta = 0$.

q	e_1^q	o_1^q	e_2^q	o_2^q	e_3^q	o_3^q	e_4^q	o_4^q	e_5^q	o_5^q	e_6^q	o_6^q
5	$2.2540e-04$	-	$4.3785e-05$	-	$1.1494e-05$	-	$2.3057e-08$	-	$6.2325e-08$	-	$1.1981e-07$	-
6	$2.5893e-05$	3.12	$5.1171e-06$	3.10	$1.3371e-06$	3.10	$6.0856e-11$	8.57	$3.7701e-11$	10.69	$1.0798e-10$	10.12
7	$4.4945e-04$	-4.12	$3.7303e-04$	-6.19	$8.4739e-05$	-5.99	$3.6913e-12$	4.04	$2.3932e-12$	3.98	$1.3776e-12$	6.29
8	$4.4035e-07$	10.00	$3.5802e-07$	10.03	$7.3336e-09$	13.50	$1.0836e-13$	5.09	$9.5923e-14$	4.64	$8.0380e-14$	4.10
9	$4.5085e-08$	3.29	$8.8880e-09$	5.33	$2.3887e-09$	1.62	$2.2204e-15$	5.61	$3.9968e-15$	4.58	$1.7764e-15$	5.50

Table 8: Grid refinement analysis for the classical WENO method for $r = 4$ algorithm for the function in (40) for f_0, i.e. $\eta = 0$.

q	e_1^q	o_1^q	e_2^q	o_2^q	e_3^q	o_3^q	e_4^q	o_4^q	e_5^q	o_5^q	e_6^q	o_6^q
5	$2.2758e-04$	-	$8.2213e-06$	-	$8.3659e-07$	-	$1.4049e-07$	-	$2.0247e-08$	-	$1.5088e-07$	-
6	$2.6096e-05$	3.12	$4.5246e-07$	4.18	$2.5666e-08$	5.03	$3.1740e-09$	5.47	$3.1643e-09$	2.68	$2.9024e-09$	5.70
7	$2.9276e-06$	3.16	$2.8320e-08$	4.00	$7.4517e-10$	5.11	$4.3556e-11$	6.19	$4.6446e-11$	6.09	$4.8595e-11$	5.90
8	$3.7307e-07$	2.97	$1.5179e-09$	4.22	$2.5495e-11$	4.87	$5.6133e-13$	6.28	$5.9375e-13$	6.29	$6.2617e-13$	6.28
9	$4.5639e-08$	3.03	$9.1202e-11$	4.06	$8.1535e-13$	4.97	$7.5495e-15$	6.22	$6.2172e-15$	6.58	$8.8818e-15$	6.14

Table 9: Grid refinement analysis for the new WENO method for $r = 4$ algorithm for the function in (40) for f_0, i.e. $\eta = 0$.

q	e_1^q	o_1^q	e_2^q	o_2^q	e_3^q	o_3^q	e_4^q	o_4^q	e_5^q	o_5^q	e_6^q	o_6^q
5	$1.8881e+02$	-	$2.7044e+01$	-	$3.8405e-06$	-	$2.9591e-06$	-	$1.5404e-06$	-	$3.9272e-07$	-
6	$3.7462e+02$	-0.99	$5.3588e+01$	-0.99	$2.6340e-07$	3.87	$2.5774e-07$	3.52	$2.4316e-07$	2.66	$2.1983e-07$	0.84
7	$7.4624e+02$	-0.99	$1.0668e+02$	-0.99	$1.6297e-08$	4.01	$1.6477e-08$	3.97	$1.6513e-08$	3.88	$1.6406e-08$	3.74
8	$1.4930e+03$	-1.00	$2.1335e+02$	-1.00	$9.8526e-10$	4.05	$9.9893e-10$	4.04	$1.0103e-09$	4.03	$1.0194e-09$	4.01
9	$2.9865e+03$	-1.00	$4.2671e+02$	-1.00	$6.0034e-11$	4.04	$6.0590e-11$	4.04	$6.1111e-11$	4.05	$6.1589e-11$	4.05

Table 10: Grid refinement analysis for the linear Lagrange method for $r = 3$ algorithm for the function in (40) for f_{10}, i.e. $\eta = 10$.

q	e_1^q	o_1^q	e_2^q	o_2^q	e_3^q	o_3^q	e_4^q	o_4^q	e_5^q	o_5^q	e_6^q	o_6^q
5	$2.2187e-03$	-	$5.1191e-04$	-	$4.9491e-06$	-	$4.7419e-06$	-	$2.6510e-06$	-	$2.1599e-06$	-
6	$5.2818e-04$	2.07	$1.1285e-04$	2.18	$2.6489e-07$	4.22	$2.9352e-07$	4.01	$3.1452e-07$	3.08	$3.2063e-07$	2.75
7	$1.2891e-04$	2.03	$2.6612e-05$	2.08	$1.4689e-08$	4.17	$1.5617e-08$	4.23	$1.6576e-08$	4.25	$1.7520e-08$	4.19
8	$3.1347e-05$	2.04	$6.3658e-06$	2.06	$8.4033e-10$	4.13	$8.6444e-10$	4.18	$8.9040e-10$	4.22	$9.1788e-10$	4.25
9	$7.7296e-06$	2.02	$1.5575e-06$	2.03	$5.0505e-11$	4.06	$5.1136e-11$	4.08	$5.1804e-11$	4.10	$5.2511e-11$	4.13

Table 11: Grid refinement analysis for the classical WENO method for $r = 3$ algorithm for the function in (40) for f_{10}, i.e. $\eta = 10$.

q	e_1^q	o_1^q	e_2^q	o_2^q	e_3^q	o_3^q	e_4^q	o_4^q	e_5^q	o_5^q	e_6^q	o_6^q
5	$2.2187e-03$	-	$6.5048e-05$	-	$1.0293e-05$	-	$1.8900e-05$	-	$3.2851e-05$	-	$5.3130e-05$	-
6	$5.2818e-04$	2.07	$6.3719e-06$	3.35	$3.4382e-07$	4.90	$4.7387e-07$	5.32	$6.5198e-07$	5.65	$8.9250e-07$	5.90
7	$1.2891e-04$	2.03	$7.0503e-07$	3.18	$1.5543e-08$	4.47	$1.8318e-08$	4.69	$2.1531e-08$	4.92	$2.5284e-08$	5.14
8	$3.1347e-05$	2.04	$7.9345e-08$	3.15	$7.4984e-10$	4.37	$8.1986e-10$	4.48	$8.9371e-10$	4.59	$9.7210e-10$	4.70
9	$7.7296e-06$	2.02	$9.4094e-09$	3.08	$4.0669e-11$	4.20	$4.2700e-11$	4.26	$4.4769e-11$	4.32	$4.6879e-11$	4.37

Table 12: Grid refinement analysis for the new WENO method for $r = 3$ algorithm for the function in (40) for f_{10}, i.e. $\eta = 10$.

q	e_1^q	o_1^q	e_2^q	o_2^q	e_3^q	o_3^q	e_4^q	o_4^q	e_5^q	o_5^q	e_6^q	o_6^q
5	1.9943e+02	-	4.3171e+01	-	5.4088e+00	-	1.1512e−07	-	1.1023e−07	-	1.0457e−07	-
6	3.9585e+02	−0.99	8.5642e+01	−0.99	1.0718e+01	−0.99	1.9137e−09	5.91	1.8731e−09	5.88	1.8353e−09	5.83
7	7.8871e+02	−0.99	1.7058e+02	−0.99	2.1335e+01	−0.99	3.0962e−11	5.95	3.0591e−11	5.94	3.0230e−11	5.92
8	1.5781e+03	−1.00	3.4127e+02	−1.00	4.2671e+01	−1.00	4.9560e−13	5.97	4.9072e−13	5.96	4.8894e−13	5.95
9	3.1569e+03	−1.00	6.8263e+02	−1.00	8.5342e+01	−1.00	7.1054e−15	6.12	1.1990e−14	5.35	7.5495e−15	6.02

Table 13: Grid refinement analysis for the linear Lagrange method for $r = 4$ algorithm for the function in (40) for f_{10}, i.e. $\eta = 10$.

q	e_1^q	o_1^q	e_2^q	o_2^q	e_3^q	o_3^q	e_4^q	o_4^q	e_5^q	o_5^q	e_6^q	o_6^q
5	2.2758e−04	-	4.3853e−05	-	1.1496e−05	-	2.3057e−08	-	6.2325e−08	-	1.1981e−07	-
6	2.6096e−05	3.12	5.1258e−06	3.10	1.3372e−06	3.10	6.0856e−11	8.57	3.7701e−11	10.69	1.0798e−10	10.12
7	3.1154e−06	3.07	6.1776e−07	3.05	1.6158e−07	3.05	3.6913e−12	4.04	2.3932e−12	3.98	1.3776e−12	6.29
8	3.7307e−07	3.06	7.4306e−08	3.06	1.9486e−08	3.05	1.0836e−13	5.09	9.5923e−14	4.64	8.0380e−14	4.10
9	4.5639e−08	3.03	9.1095e−09	3.03	2.3928e−09	3.03	2.2204e−15	5.61	3.9968e−15	4.58	1.7764e−15	5.50

Table 14: Grid refinement analysis for the classical WENO method for $r = 4$ algorithm for the function in (40) for f_{10}, i.e. $\eta = 10$.

q	e_1^q	o_1^q	e_2^q	o_2^q	e_3^q	o_3^q	e_4^q	o_4^q	e_5^q	o_5^q	e_6^q	o_6^q
5	2.2758e−04	-	8.2213e−06	-	8.3659e−07	-	1.4049e−07	-	2.0247e−08	-	1.5088e−07	-
6	2.6096e−05	3.12	4.5246e−07	4.18	2.5666e−08	5.03	3.1740e−09	5.47	3.1643e−09	2.68	2.9024e−09	5.70
7	3.1154e−06	3.07	2.5939e−08	4.12	7.9466e−10	5.01	4.3556e−11	6.19	4.6446e−11	6.09	4.8595e−11	5.90
8	3.7307e−07	3.06	1.5179e−09	4.09	2.5496e−11	4.96	5.6133e−13	6.28	5.9375e−13	6.29	6.2617e−13	6.28
9	4.5639e−08	3.03	9.1202e−11	4.06	8.1535e−13	4.97	7.5495e−15	6.22	6.2172e−15	6.58	8.8818e−15	6.14

Table 15: Grid refinement analysis for the new WENO method for $r = 4$ algorithm for the function in (40) for f_{10}, i.e. $\eta = 10$.